THE EFFECTS OF GEOMETRY ON SOUND RADIATION FROM THREE-DIMENSIONAL RECTANGULAR STRUCTURES

By

GRADY WAYNE COOK

Bachelor of Science
Oklahoma State University
Stillwater, Oklahoma
1959

Master of Science
Oklahoma State University
Stillwater, Oklahoma
1964

Submitted to the Faculty of the
Graduate College of the
Oklahoma State University
in partial fulfillment of
the requirements for
the Degree of
DOCTOR OF PHILOSOPHY
May, 1973

THE EFFECTS OF GEOMETRY ON SOUND RADIATION FROM THREE-DIMENSIONAL RECTANGULAR STRUCTURES

Thesis Approved:

Richard L. Lowery
Thesis Adviser

Justin R. Boyer

Donald E. Boyd

Henry R. Selesta

N. N. Hurtham
Dean of the Graduate College

ACKNOWLEDGMENTS

During the pursuit of this study I received assistance and encouragement from numerous individuals and I would like to take this opportunity to express my heartfelt thanks to a few of them. First I am grateful to the Department of the Army for giving me the opportunity to further my education.

I am most deeply indebted to my thesis adviser, Dr. R. L. Lowery, for his wise counsel and his warm friendship that I have enjoyed. My thanks go also to Drs. D. E. Boyd, L. L. Boyer, and H. R. Sebesta for serving on my Doctoral Committee and editing this thesis.

I will long remember my colleagues in the Mechanical Engineering Department in general and the Acoustics Laboratory in particular, with special thanks to Ganesh Rajagopal, Bill Smith and Bob Maffeo for all their assistance. I am certain that I received much more knowledge than I imparted during the many stimulating discussions we had.

Finally my sincerest appreciation to my wife, Nancy, for urging me to pursue the Doctor of Philosophy degree, for her encouragement along the way, and to our children Danny and Tiffany, for their sacrifices and understanding.

TABLE OF CONTENTS

LIST OF TABLES

LIST OF FIGURES

LIST OF SYMBOLS

a - Source dimension

c - Speed of sound

F - Plate mode function

G - Plate time function

k - Wave number

P - Pressure

q - Source strength

r - Radius

v - Velocity

w - Plate displacement

W - Source power

Z - Impedance

ρ - Density

σ - Area

λ - Wave length

NOMENCLATURE

db	Decibel
DI	Directivity Index
Hz	Hertz, angular frequency in cycles/second
RMS	Root-mean-square
SPL	Sound pressure level, in decibels relative to .0002 microbars

CHAPTER I

INTRODUCTION

Sound radiation from buildings and equipment enclosures is a subject of ever increasing interest, especially considering recent noise legislation. The Occupational Health and Safety Act of 1969 limits the noise levels that employees may be subjected to and thus requires that consideration be given to equipment enclosures and locations to limit noise levels. More recent legislation dealing with noise infringement across property lines makes it desirable, in fact necessary, to predict or estimate the noise radiation patterns of structures before they are built. Specific types of equipment and shelters have been investigated on occasion as problems occurred, but there has been virtually no research conducted into the sound radiation patterns of three-dimensional rectangular sound sources in general, even though most buildings and equipment enclosures are in this category.

Sound radiation from all of the elementary classical sound sources such as spheres, ellipsoids, cylinders and pistons of different shapes, has been studied in detail and is discussed in most

acoustics texts. The sound field of vibrating plates and panels has also been studied in recent years and is discussed in some of the more recent advanced texts dealing with acoustics.

A few greatly simplified methods have been proposed for predicting the sound levels from plane two-dimensional sources based on expected acoustic power or surface intensities, but most of these are independent of frequency and seem to have only limited practical value.

To understand the complexity of the problem and the need for simplification, the basic equation for sound radiation from a vibrating surface must be considered. (Figure 1).

$$d\bar{p} = \frac{j\rho ck}{2\pi} (\bar{v} \cdot d\bar{\sigma}) \frac{e^{j(\omega t - kr')}}{r'}$$

$$\bar{p} = \frac{j\rho ck}{2\pi} e^{j\omega t} \int_s \frac{(\bar{v} \cdot d\bar{\sigma}) e^{-jkr'}}{r'}$$

Even for the relatively simple case of a piston where all points are in phase and the velocity is normal to the surface, the resulting equation is so complex that it cannot be integrated if the exact expression for r' is used.

$$\bar{V} \cdot d\bar{\sigma} = V_o \, d\sigma$$

$$r = (x^2 + y^2 + z^2)^{\frac{1}{2}}$$

$$r' = [(x - x')^2 + (y - y')^2 + z^2]^{\frac{1}{2}}$$

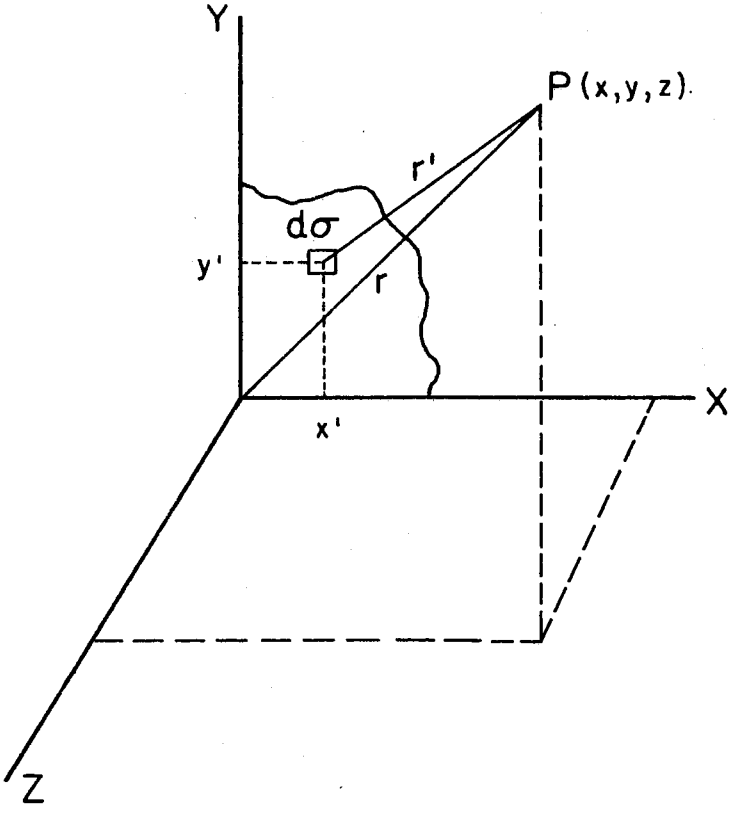

Figure 1. Geometry of Sound Radiation From a Surface.

To obtain an approximate solution, the expression for r' must be expanded binomially and only the first two terms retained. This is equivalent to restricting the point of pressure computation to a distance much greater than the size of the piston ($z \gg x$ and $z \gg y$, or $r' \approx r$).

The magnitude of the problem is even greater when the general expression for the velocity profile over a plate is examined, and the plate is a large wall such that the approximation for r is not valid (i.e., close distance).

$$\bar{v}(x, y, t) = \frac{d}{dt} [\bar{W}(x, y, t)]$$

$$W(x, y, t) = \sum_{m=1}^{\infty} \sum_{n=1}^{\infty} G_{mn}(t) \, F_{mn}(x, y)$$

$$\bar{v}(x, y, t) = \sum_{m=1}^{\infty} \sum_{n=1}^{\infty} \frac{d}{dt} [G_{mn}(t)] \, F_{mn}(x, y)$$

It is readily obvious that the resulting expression would certainly not be integrable if the expression above were put in the general equation for pressure. According to Skudrzyk (1), "The exact computation of the sound field of a complex vibrator is a difficult and laborious task--if it is possible at all. Even if this computation were possible, it is doubtful whether the result would be worth the trouble."

The preceding discussion is only for the case of a plane, two-dimensional surface. The complexity is greatly increased when five such plane surfaces are arranged in three-dimensions to form a "building". In addition to the sound radiation from each "visible" surface, consideration must also be given to the diffraction of the sound waves around the corners.

There is currently no satisfactory method to accurately predict such things about sound radiation from buildings as directivity patterns and where spherical spreading begins.

The purpose of this research was therefore to initiate the general study of sound radiation from three-dimensional rectangular structures and determine whether a relationship exists between sound radiation and source geometry independent of structure dynamic properties. Specifically, the two primary objectives of this research were to:

(1) Determine how geometry alone affects the directivity patterns of sound being emitted from a three-dimensional rectangular source.

(2) Determine how geometry alone affects the decrease of sound pressure level with distance relatively near the source.

The investigation of the subject was conducted in three distinct experimental phases, which were:

(1) Experiments in the anechoic chamber with small scale models.

(2) Experiments out-of-doors with large scale models.

(3) Experiments with surface gravity waves on a water table.

The scope of this research was limited to measurements in two-dimensions, in the horizontal plane, about a three-dimensional sound source. A three-dimensional directivity pattern was not included in this study. The study was also limited to rectangular structures of wooden construction with length-width-height ratios of .6-1-1 to 2.1-1-1. It did not include very elongated models in either the vertical or horizontal dimension.

CHAPTER II

LITERATURE REVIEW

The literature dealing directly with the subject of this investigation was virtually nonexistent and even literature dealing with it indirectly was scarce. Generally the literature that was reviewed can be divided into three categories:

(1) Investigations of specific noise radiation problems.

(2) Study of the sound field of plates and panels.

(3) Proposed methods of predicting the sound pressure levels from plane, two-dimensional sources.

Investigation of Specific Areas

Noise radiation from large electrical power transformers into surrounding communities caused some concern in the 1950's and prompted several studies. Johnson et. al. (2) used scale models in a study of this subject and achieved good correlation between scale model and full size data by plotting noise reduction versus a "dimensionless distance" (Figure 2). This normalized distance was the quotient of the true distance and the square root of the visible surface area.

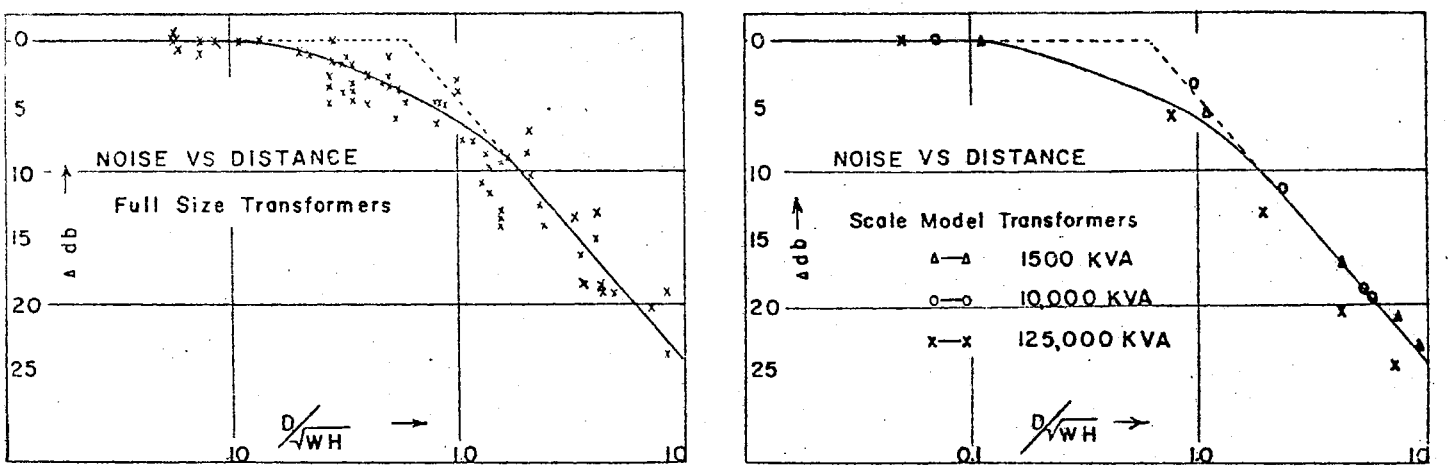

Figure 2. Noise Versus Distance, Electrical Transformers

Studies have been made on cooling tower noise also. R. M. Ellis (3) studied the sound radiation from large circular natural draft cooling towers and was able to predict with very good accuracy the noise level as a function of geometry.

The circular cooling towers were comparatively simple sound sources as shown in Figure 3 being basically open "cylinders" of radius R and height h'. The sound was relatively broad band noise and was logically assumed to behave as a circular array of an infinite number of incoherent sources. Ellis made the following assumptions:

(1) The radiation pattern would remain circular.

(2) The sound level at any point could be determined as a function of the power or intensity and independent of frequency.

(3) The inward radiated sound does not "escape" so that the SPL at any point was a function only of the "visible" portion of the cylinder as shown in Figure 4. (e.g. diffraction was neglected.)

A straightforward relationship was derived to estimate the sound pressure at any point based on total acoustic power, and then an empirical relationship was developed to predict the acoustic power as a function of the tower geometry and mass flow rate of cooling water. This empirical model was based on measurements of the sound radiation from existing cooling towers.

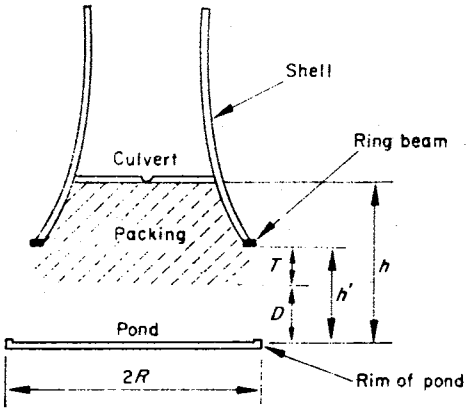

Figure 3. Typical Cooling Tower Construction

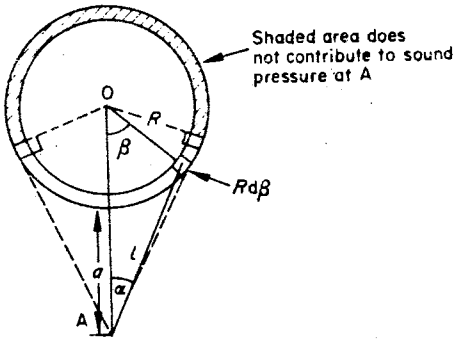

Figure 4. Sound Radiation From a Ring Source

Sound Fields of Plates

The literature dealing with sound and plates can be divided into three broad categories:

(1) Plate response to sound and boundary layer excitation.

(2) Transmission of sound through thin plates.

(3) Acoustic power radiation from vibrating plates.

Most of the literature was more abstract than desired for this research since detailed knowledge of the plate structural properties was necessary. It was felt that the truly general method sought must be independent of wall dynamics. Papers on the two subjects of primary concern to this research (i.e., source geometry effects on directivity patterns and farfield distances) were almost totally absent from the literature.

K. Gosele (4) derived some relationships for a "radiation factor" which he defined as the ratio of the sound power radiated from a vibrating plate to the sound power of a plate of the same size vibrating rigidly (e.g. a piston). He derived a directivity function for radiated energy in the special case of a traveling wave which showed that for frequencies at or below the coincidence frequency the radiated energy is concentrated on the axis of symmetry, but at frequencies above the critical frequency, the lobe of radiated energy is moved to some angle off this axis. It further showed that the

sharpness of the lobes is a function of the size of the plate. A traveling wave is not of practical concern however.

Cremer and Heckl (5) elected to use an approximation of a vibrating plate, rather than attempt to integrate Kirchoff's integral with the exact plate velocity profile. They assumed that a rectangular plate vibrating in the m by n mode can be modeled as an m by n array of simple sources distributed at equal intervals over the plate. Each source is assumed to be of equal strength ($q_i = vd\sigma$) and adjacent sources 180 degrees out of phase. The relationship is made very simple by making the (a, b) source in the array.

$$q_{ab} = (-1)^{a+b} q_i$$

$$q_{ab} = e^{-j(a+b)\pi} q_i$$

With this relationship, Kirchoff's integral reduced to the product of two series summations which was quite suitable for programming on a digital computer.

The radiation patterns are plotted for several cases, which show two primary lobes of sound radiation at approximately $\pm \pi/4$ off the axis of symmetry. The magnitude of the lobes is a function of the source size (ka) and array size. The larger the array size, of course, the greater the number of minor lobes. (Figure 5)

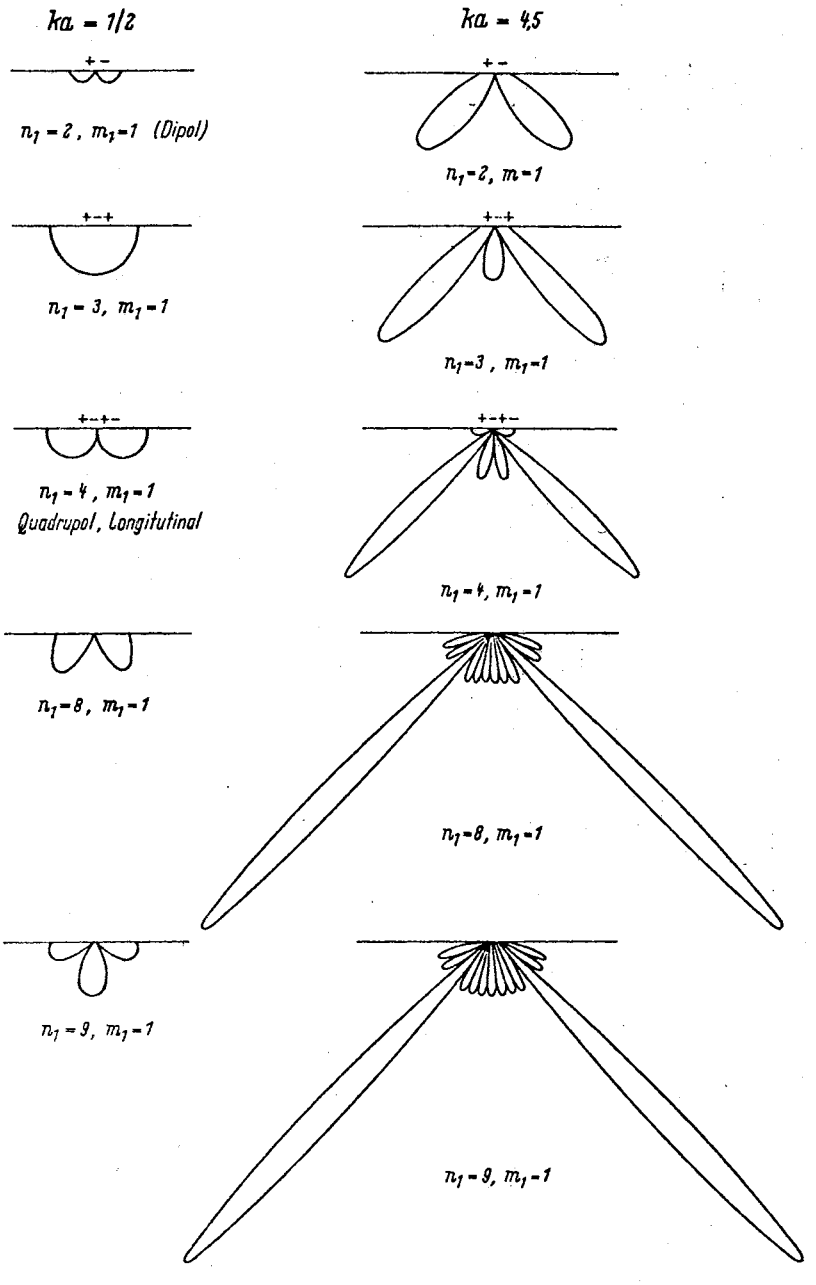

Figure 5. Directivity Patterns of Linear Arrays of Dipoles

Finite Plane Sound Sources

The other methods found that attempted to predict radiation patterns were all based on sound intensity independent of frequency, and the assumption that a plane source behaves as an infinite array of incoherent sources.

E. Rathe (6) used the fundamental relationship

$$(P_{RMS})^2 = WZ/4\pi r^2$$

and treated the plane source as an infinite array of small elementary sources. He asserted that the effective pressure squared at a point on the axis of symmetry is equal to the integral of all the elemental sources over the entire plane surface. By straightforward integration he arrived at an approximation for the SPL attentuation with distance.

R. Ellis (7) pointed out a rather insignificant error at close distances in Rathes paper. He then expanded the work to include other points than on the axis of symmetry, such as on a line perpendicular to the edge and at an angle to the edge and presented some db correction curves for the close distance errors. By using several of these points one can approximate a frequency independent radiation pattern and an estimate of the farfield distance.

R. Tatge (8) proceeded in a very similar manner to both of the above, but like Rathe, only for the axis of symmetry. His results were given essentially as a series of plots of db corrections for various cases.

In another recent paper, Z. Maekawa (9) claimed to base his calculations on the total energy density, but in actuality he omitted the kinetic energy density term, $\frac{1}{2} \rho_o v^2$, so in fact also used sound intensity. One of his methods was a little more general than the preceding ones as it approximated the intensity at any point in front of a plane surface by a summing process. However, it involved use of a chart (to determine the value of a numerically evaluated integral) which was valid only at distances closer than approximately one wall width. Another of his methods gave some consideration to surface directivity (his first method did not), but again only on the axis of symmetry.

CHAPTER III

THE EXPERIMENTAL METHODS

The investigation of this subject was divided into three distinct phases, each with a different experimental procedure. They were, in the order they were performed:

(1) Small scale model experiments.

(2) Large scale model experiments.

(3) Water table experiments.

Small Scale Model Experiments

It was decided to conduct the initial investigations with small scale models because of the availability of the anechoic chamber at Oklahoma State University which would simulate a free field environment and eliminate the uncontrollable variables such as wind, humidity and temperature gradients. The anechoic chamber was approximately 17 feet by 22.5 feet measured from the points of the wedges, with a wedge depth of 9 inches. This wedge depth gave a theoretical cutoff frequency of 375 Hz, below which there should be no reflection and hence no echos or standing waves. The background noise in all

octave bands from 500 Hz and up was below 20 db, and from the 250 Hz band and down was usually below 25 db.

An ordinary antenna rotor was suspended from the ceiling to rotate a boom in a circular arc, from which the microphone was suspended. The rotor and control box were designed such that rotation was accomplished in six degree increments which was therefore the minimum rotation possible between measuring points. The rotor control box and all instrumentation were remotely located outside the chamber. The actual instrumentation used for measuring the SPL is listed in the appendix.

The models were built to 1/10 scale of an 8 foot high by 8 foot wide by 11.3 foot long enclosure, thus making them 9.6 inches by 9.6 inches by 13.6 inches. They were constructed of three-quarter inch plywood so the walls would be effectively infinitely rigid when compared to the interior volume of the models and the acoustic pressures inside. Five variations were constructed in addition to the basic solid walled model.

The end was made removable in one variation so that ends of different material could be installed, and a side was made removable in a second variation for the same reason. The three remaining models had one or more walls perforated with a rectangular array of .125 inch holes on one inch centers covering the entire wall(s). One had a perforated end only, another a perforated end and side, and the last a perforated end, side and top.

The sound source inside the models was a very high frequency high fidelity loudspeaker driven by an audio power amplifier with an input signal from a random noise generator. Details of the equipment used are in the appendix.

A reflecting plane to simulate the ground was created with acoustical ceiling tile by placing it on the wire floor of the anechoic chamber. The test model was placed on this surface and centered under the boom rotor. The microphone was positioned manually in the horizontal plane of interest and at the desired radius from the center of the source.

Sound-level measurements were made in seven planes to get a three-dimensional sound radiation pattern. In each of these planes, readings were taken at nine different radii from 3.25 to 60 inches and at nine different azimuths. Thus, there was a grid of 81 discrete points in each of the seven planes where measurements were taken for each of the test models.

At each of these grid points, the A-weighted SPL readings were taken as well as 1/3 octave band readings at 1, 2, 4, 8, and 16 Kilohertz. The lower of these frequencies was chosen because of the desire to stay above the cutoff frequency of the chamber, and because of the speaker frequency response. The upper frequency was dictated only by the capability of the speaker. Based on the 1/10 scale size of the models these frequencies correspond to full

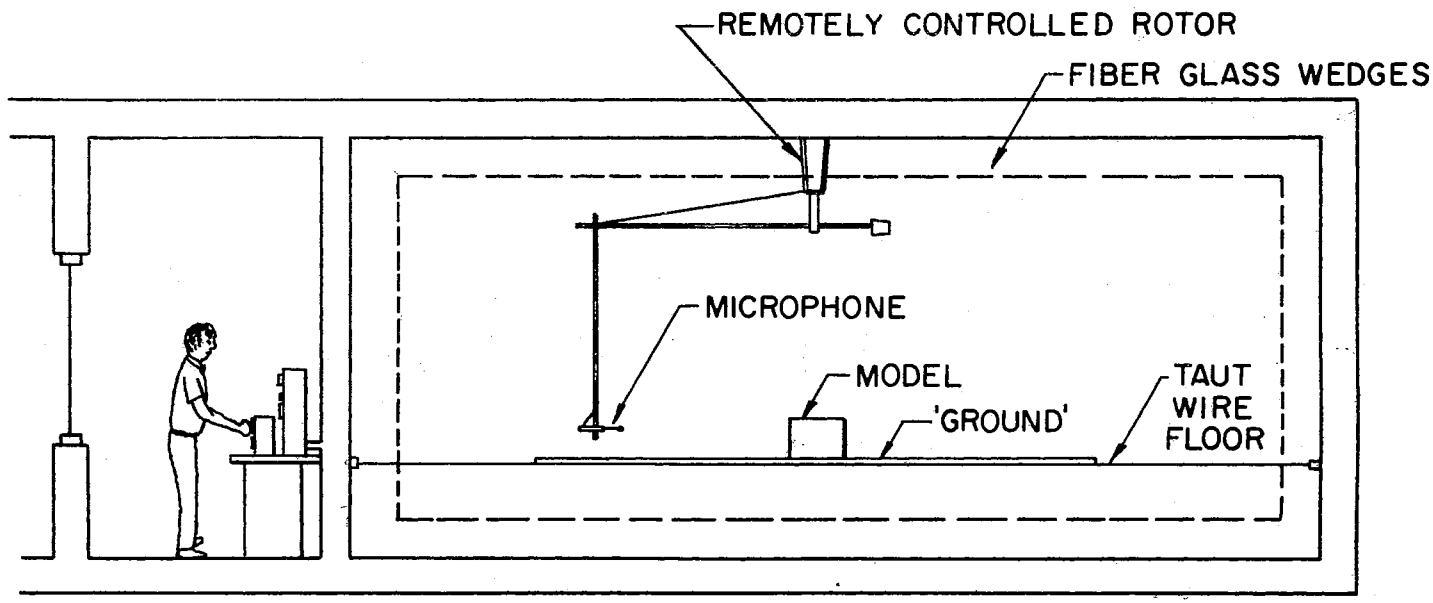

Figure 6. Anechoic Chamber Test Arrangement

size frequencies of 100 to 1600 hertz, which was felt to be a sufficiently wide frequency range.

The equipment requiring calibration was calibrated in accordance with the operating or maintenance manuals. The frequency analyzer was completely calibrated separately and then the microphone and frequency analyzer were calibrated together with a pistonphone. It was determined that the calibration factor, K, for the microphone being used was 31.6 db rather than 35.1 db specified on the calibration sheet provided with the microphone. Age and use could account for this change in sensitivity. Constant errors, such as the value of K above, though corrected, were of minimal concern since all results were being normalized with respect to the zero degree azimuth readings.

Large Scale Model Experiments

The instrumentation used for the large scale model experiments was in general somewhat less extensive than that used for the small scale model experiments. The actual SPL measurements were taken with a portable sound level meter which was equipped with an octave band filter set, (see appendix). However, the same equipment used in the small scale model experiments was used to measure and plot the continuous frequency spectrum near the source in one case. The sound level meter was calibrated daily with a pistonphone when measurements were being taken.

The large scale model was constructed of one-half inch plywood with 2 by 4 studs on 2 foot centers. The width and height dimensions were fixed at 8 feet each and the length was made variable from 4.67 feet to 16.67 feet by the insertion of 4 foot wide prefabricated panels. Thus, there were in effect four full size models of different lengths. The sound source inside the models was a high efficiency loud speaker system, powered by the same audio power amplifier and random noise generator as the small scale models. An audio oscillator was used as the signal generator for some pure tone tests.

The large models were erected on a flat, remote location at the Stillwater Municipal Airport. They were positioned approximately 400 feet from the only nearby hanger, and at a slight angle to minimize reflections and standing waves. A large polar coordinate grid system was laid out around the models. Complete 90 degree arcs were made at radii of 26, 58, 106, and 154 feet with grid points at every ten degrees on these arcs. Additionally, on the axis of the two walls (zero and 90 degrees) grid points were placed at every 8 foot interval. The only vegetation on the site was common grass which was maintained at a height of approximately four inches throughout the experiments.

The sound level meter was tripod mounted at a height of 48 inches (the plane through the center of the source) and SPL readings taken for the A-weighted level, 250, 500, 1000, 2000 and 4000 Hz

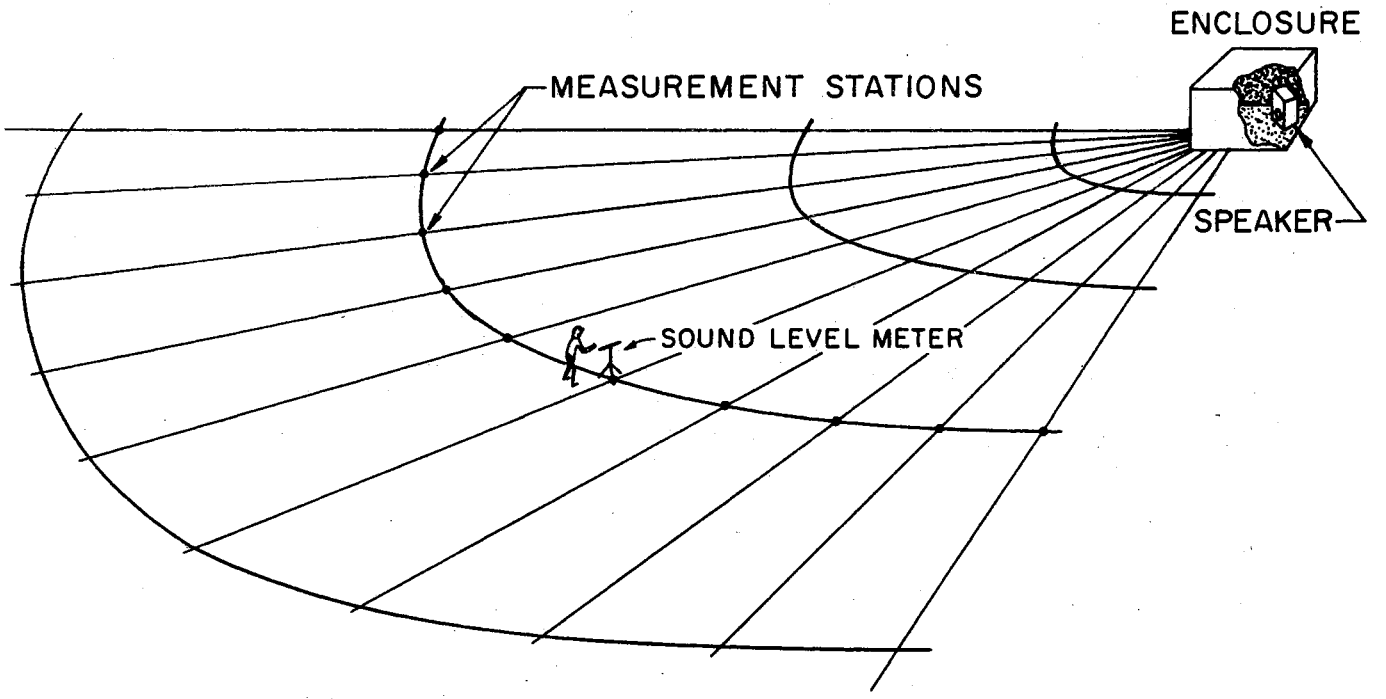

Figure 7. Large Scale Model Test Arrangement

octave bands at all of the grid points. For one model, readings were also taken at heights of 30 and 90 inches.

The flat remote location was selected for two reasons. First it was necessary to locate the models away from other structures as mentioned for a free-field. Secondly, it was necessary to have a site where the residual background noise level was sufficiently low to be insignificant while taking measurements. The site selected was adequate in both respects. Background levels were typically below 35 db in the 250 Hz through 1000 Hz octave bands and below 30 db in the 2000 Hz and 4000 Hz octave bands, and frequently below 30 db and 25 db, respectively. Background levels were checked frequently throughout the periods when measurements were being taken to ensure that there was always an absolute minimum of ten db difference between the background level and the lowest SPL's being measured. Normally the minimum difference was between 15 to 20 db. When two signals are being added that have a difference of ten db, the result is less than .5 db greater than the larger and if the difference is greater than 15 db the result is less than .1 db greater than the larger.

In addition to being cautious with the background levels, weather conditions were also watched very closely. Wind and temperature gradients are significant factors usually only at much greater distances than those involved in this research. Nevertheless,

it was desired to minimize these variables as much as possible. Therefore, data was generally taken only during the morning hours on calm days with less than about five miles per hour wind speed. Several days were required to complete the data gathering for each model, but all the data for a given arc or a given axis was taken on the same day.

In addition to the large scale models, the directivity pattern from a large newly constructed steel building was measured before any interior partitions were installed. The same sound source and measuring techniques were used as with the large scale models.

Water Table Experiments

Experiments with a water table were included in the study to gain further understanding of the sound radiation patterns, by visually studying water gravity waves. A water table was designed and built 29.5 inches square and 2.25 inches deep. The sides were lined with removable one inch thick cotton pads, contained in screen wire, to reduce reflection and thus standing waves.

Several wave generators (drivers) were built and tested. The first were essentially pistons (entire surface in phase) operated by a four-bar mechanism which generated plane waves on the surface. Unfortunately they were relatively low frequency (below ten Hz) and generated a series of impulses rather than continuous waves. Two

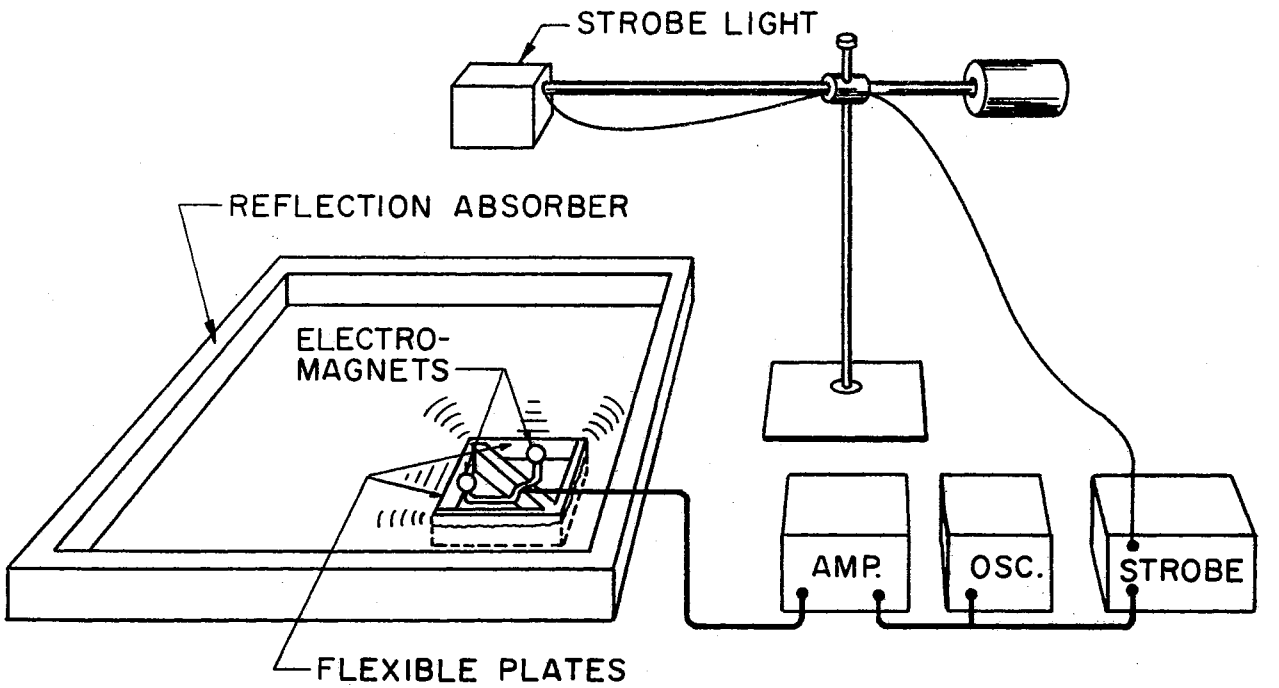

Figure 8. Water Table Test Arrangement

other drivers capable of relatively high frequency were then built and proved to be more satisfactory. One consisted of two, 2 inch by 6 inch oval loudspeakers mounted on adjacent sides in a square box. They were waterproofed and immersed directly in the water table. The most satisfactory driver was built with two stainless steel membrane "ribbons" and two electromagnets for exciters. The electromagnets were powered by an ordinary audio power amplifier with an input from an audio oscillator.

The procedure was simply to immerse the wave generator in the water table, slowly sweep the audio oscillator through the frequency range of interest, observe and photograph the wave radiation patterns. Observation and photography of the waves was accomplished with the aid of a stroboscopic light.

CHAPTER IV

EXPERIMENTAL RESULTS

The papers by Maekawa (9) and Ellis (7) indicated that a single plane radiating surface would have one large primary lobe on its axis and no side lobes of any significance. The initial objective of the experimental study was therefore intended to determine more closely the directivity pattern from a single radiating wall. Logically then, the radiation pattern from multiple radiating surfaces could be obtained by combining the individual directivity patterns. The preliminary experimental work disproved this theory rather quickly however.

Small Scale Model Results

Directivity Patterns

The initial small scale model experiments were conducted with the model with the removable end and several ends of different material, lighter than the three-quarter inch plywood were used. Since the lighter end would not afford as much noise reduction, it would have greater intensity on the outside than the other walls and

thus radiate more power. This proved to be the case and rather large lobes were measured on axis for each of the materials experimented with as shown in Figures 9 through 14. Figure 9 is the 1/3 octave band pattern at 1000 Hz from a wall of .009 inch thick aluminum sheet. Likewise, Figure 10 is the 1000 Hz, 1/3 octave band pattern for .25 inch plasterboard (sheetrock), and Figure 13 is the 1000 Hz, 1/3 octave band pattern from a wall of perforated masonite (pegboard). Figures 11, 12 and 14 show the 8000 Hz, 1/3 octave band patterns for the same three materials. All of these patterns are typical and only intended to be a representative sample.

It is not considered particularly meaningful to discuss a directivity index (DI) of a "building" in general since there must be a reference axis to define a DI. Additionally, by definition, a simple point source in an infinite baffle (such as on the ground) radiating uniformly into a hemisphere already has a DI of 2 by definition even though it is omnidirectional in the hemisphere. The confusion is further compounded in this case since the "plane" source is really radiating into a quarter-sphere and again by definition, would have a directivity index of 4, even if it were perfectly omnidirectional within this quarter-sphere. It is therefore, probably more illustrative to discuss "beam-width". Thus, the walls just discussed have six db beam-widths of approximately 75, 65 and 105 degrees respectively for 1000 Hz, and 70, 50 and 150 degrees for 8000 Hz.

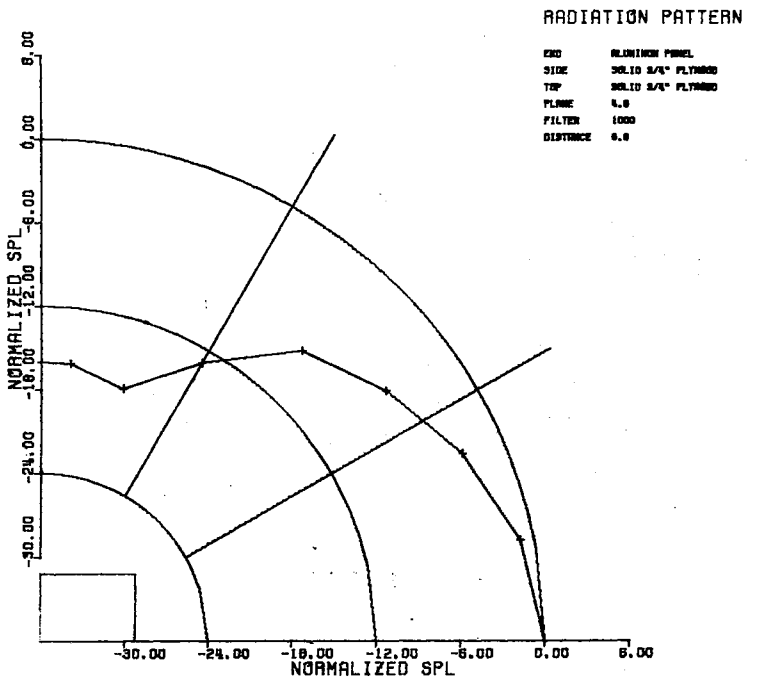

Figure 9. Directivity Pattern of Small Scale Model (1/3 Octave Band at 1000 Hz with .009" Aluminum End)

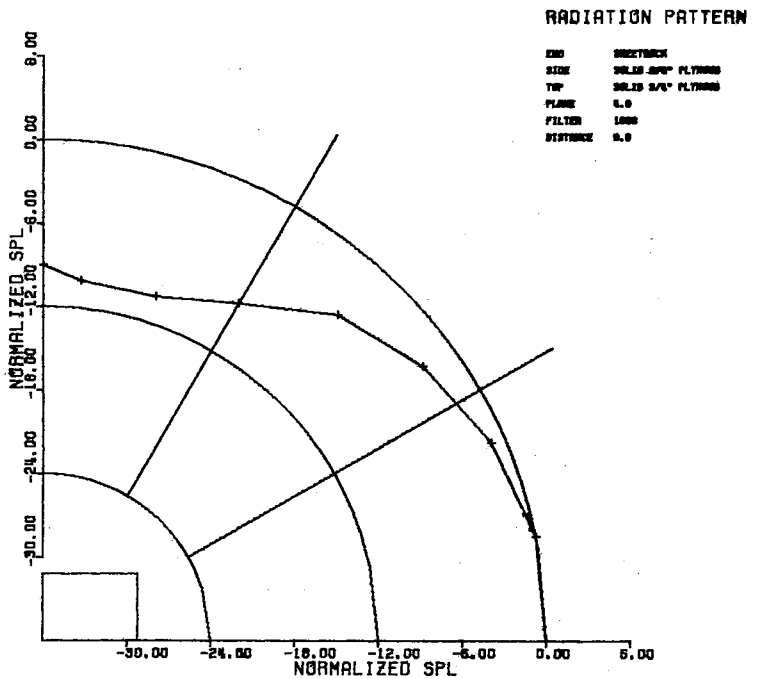

Figure 10. Directivity Pattern of Small Scale Model (1/3 Octave Band at 1000 Hz with .25" Sheetrock End)

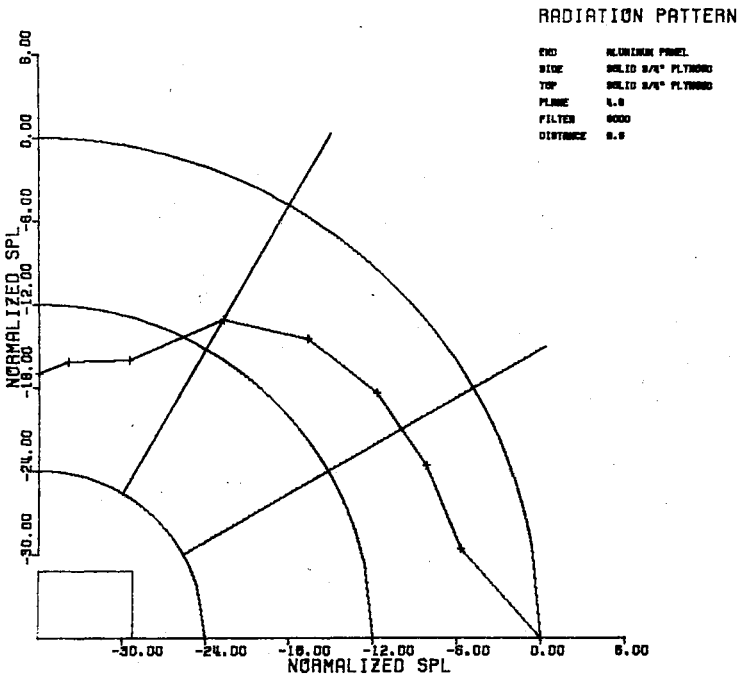

Figure 11. Directivity Pattern of Small Scale Model (1/3 Octave Band at 8000 Hz with .009" Aluminum End)

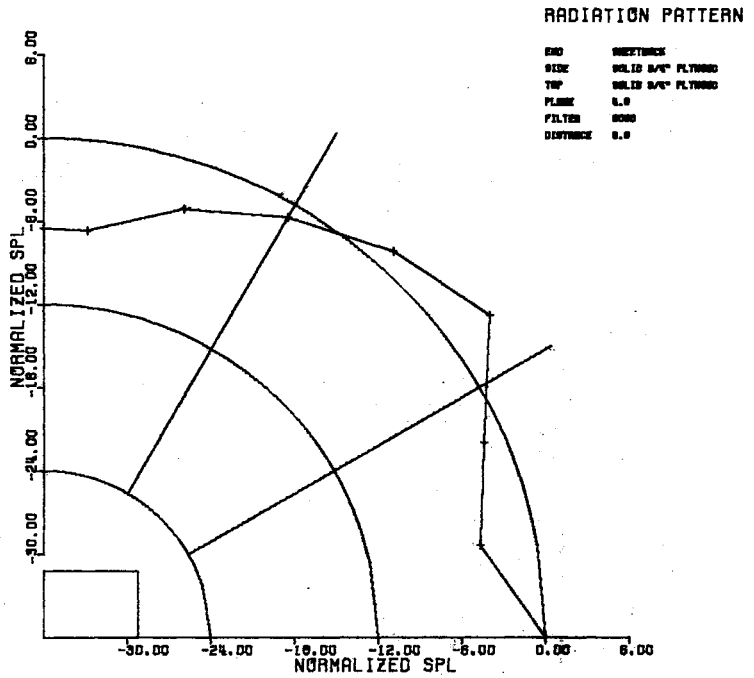

Figure 12. Directivity Pattern of Small Scale Model (1/3 Octave Band at 8000 Hz with .25" Sheetrock End)

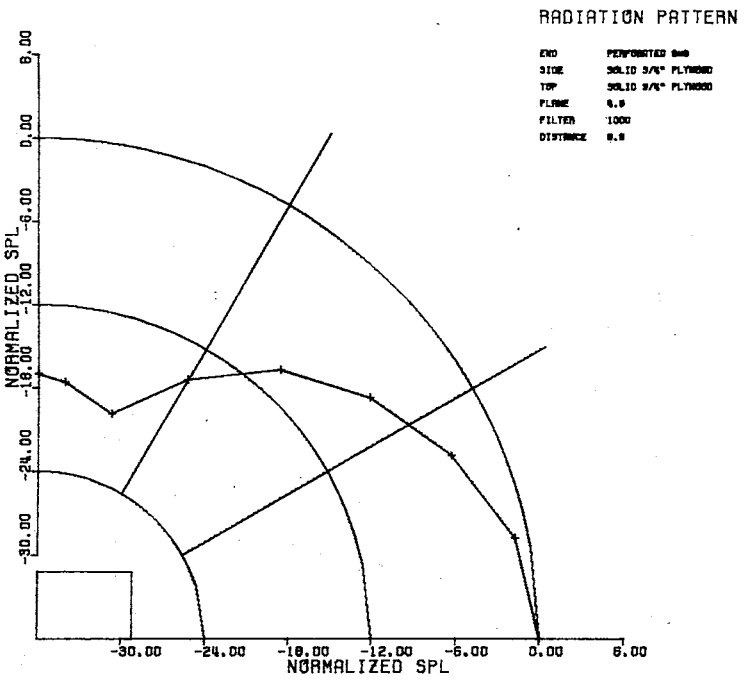

Figure 13. Directivity Pattern of Small Scale Model (1/3 Octave Band at 1000 Hz with Pegboard End)

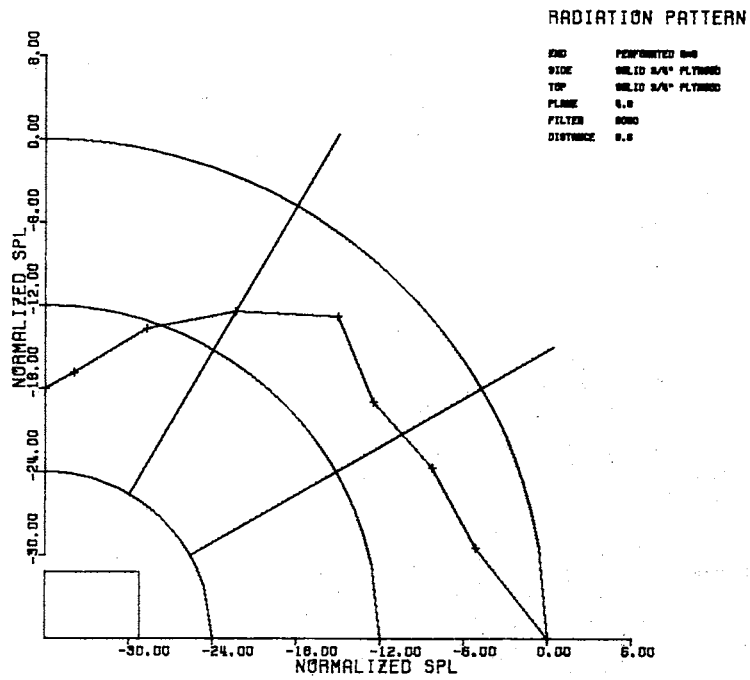

Figure 14. Directivity Pattern of Small Scale Model (1/3 Octave Band at 8000 Hz with Pegboard End)

Figures 15 and 16 show the directivity patterns for the model with the nine by nine array of perforations on the end and it exhibits very similar patterns to the other "single wall" sources. They have six db widths of 50 and 100 degrees for 2000 and 8000 Hz respectively.

When the second wall (the side) was perforated with a similar array of holes to simulate two radiating walls, very wide and strong corner lobes appeared as shown in Figure 17 for 1/3 octave at 2000 Hz. The magnitude of these corner lobes varied from 6.5 db at 2000 Hz to zero db at 4000 Hz. Perforation of the third wall (the top) had no measurable affect on the directivity patterns in planes below the plane of the top.

The measured directivity patterns of the scale model with all solid sides also had wide strong corner lobes, similar to those in the preceding case, as shown in Figures 18 and 19. This result led to the conclusion that the radiation pattern was more strongly dependent on geometry than on the properties of the walls. The magnitude and size of the lobes in the case of the solid walled model varied from as little as zero db at 2000 Hz to nearly seven db at 4000 Hz.

SPL Decrease With Distance

The decrease of sound-pressure-level with distance was not quite as well behaved as the inverse distance squared law predicted and varied considerably from one frequency to the other, as can be

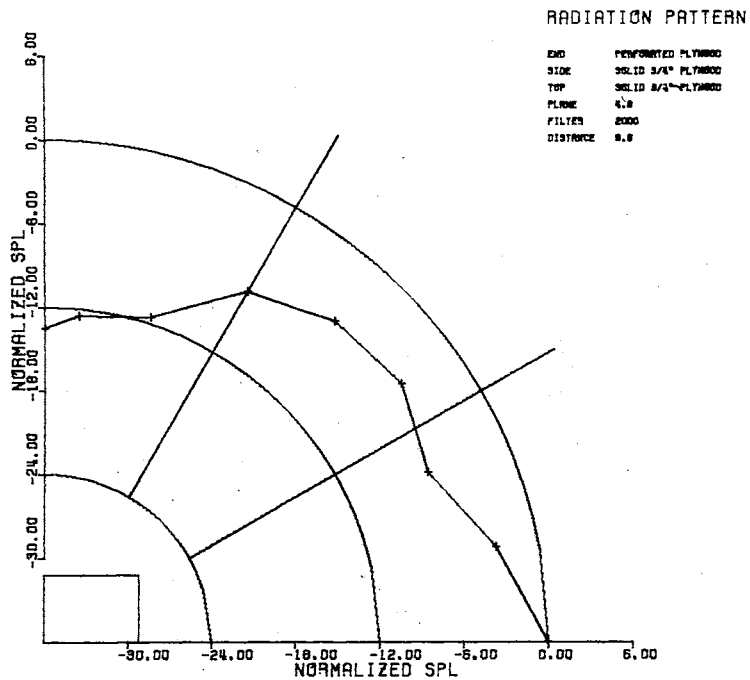

Figure 15. Directivity Pattern of Small Scale Model (1/3 Octave Band at 2000 Hz with Perforated Plywood End)

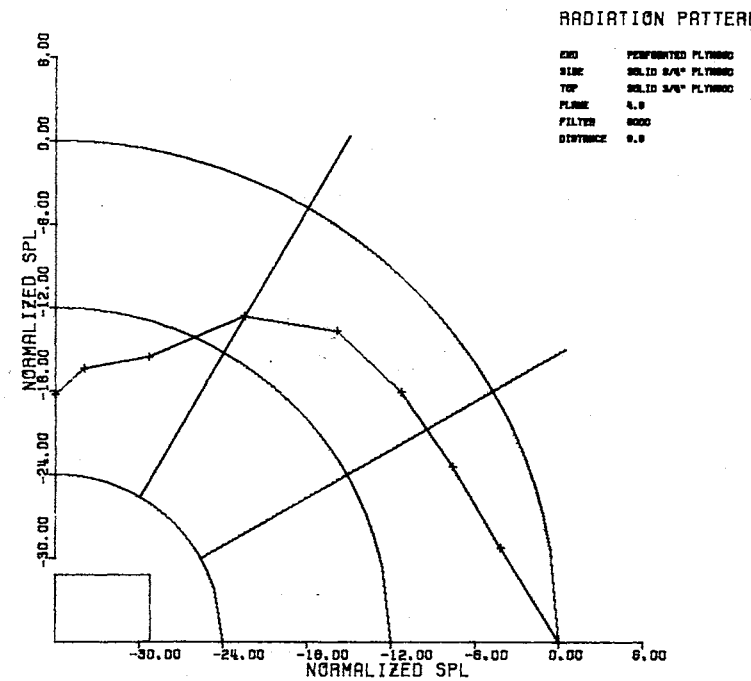

Figure 16. Directivity Pattern of Small Scale Model (1/3 Octave Band at 8000 Hz with Perforated Plywood End)

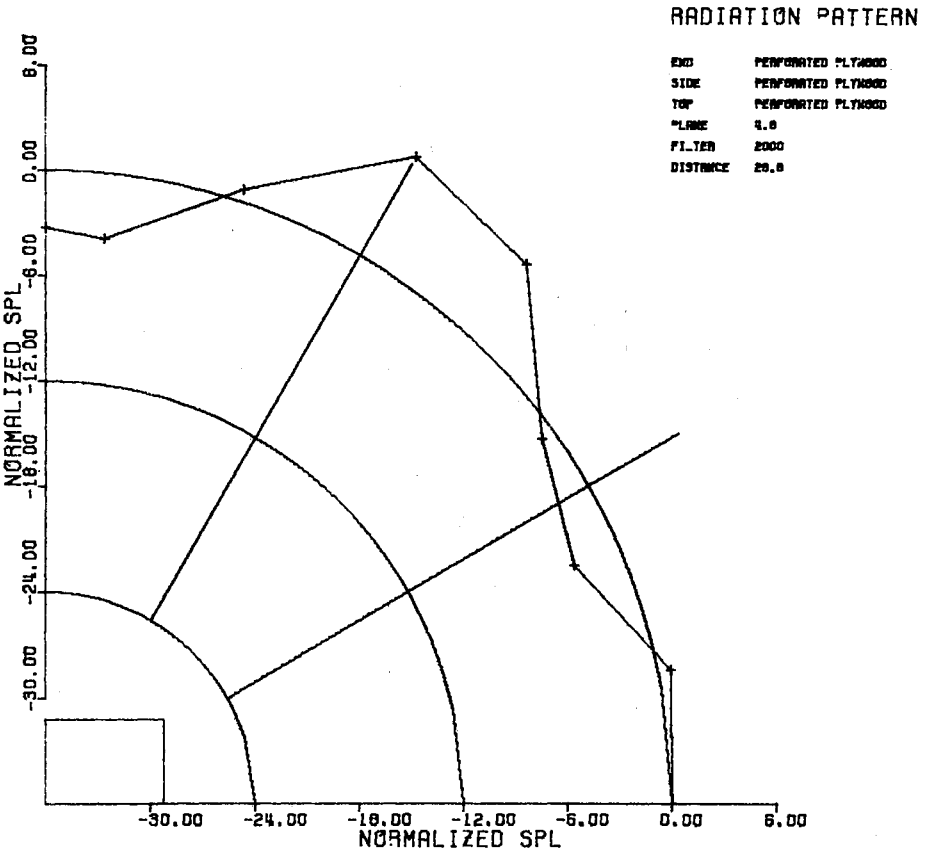

Figure 17. Directivity Pattern of Small Scale Model (1/3 Octave Band at 2000 Hz with All Sides Perforated)

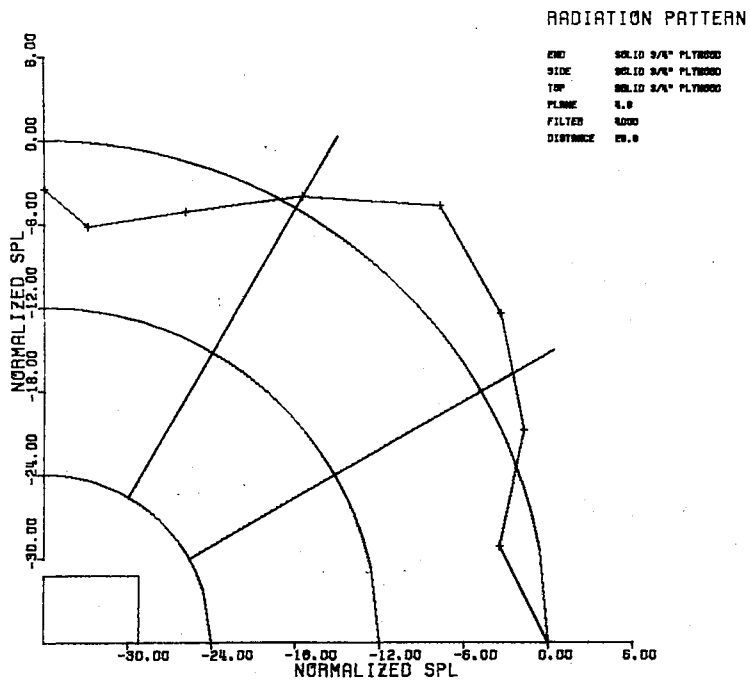

Figure 18. Directivity Pattern of Small Scale Model (1/3 Octave Band at 4000 Hz with all Solid Walls)

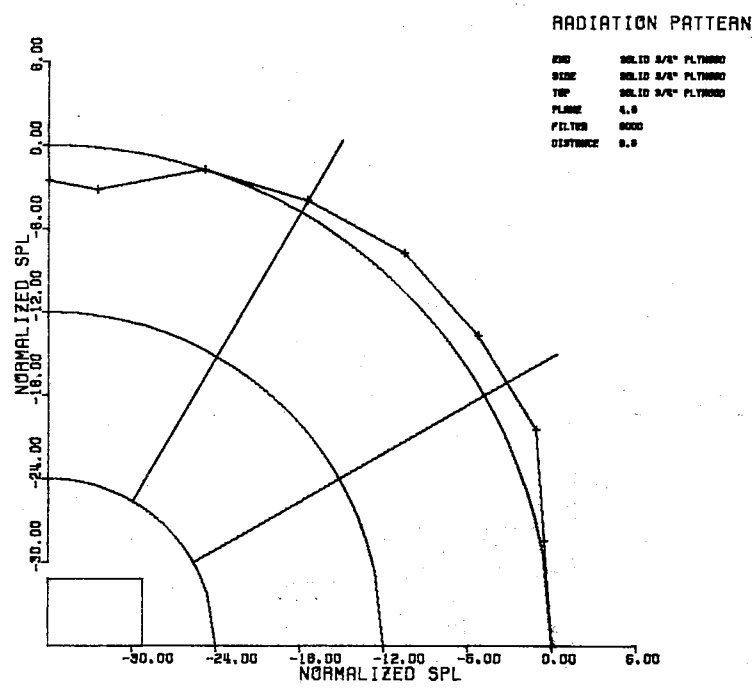

Figure 19. Directivity Pattern of Small Scale Model (1/3 Octave Band at 8000 Hz with all Solid Walls)

seen in Figures 20 and 21. The lower frequencies began to conform to the minus six db slope (per doubling of distance) as close as one or two wall widths (Figure 20), a wall width being defined as the horizontal dimension of the radiating surface. The higher frequencies, however, often did not conform to the minus six db slope until a distance of five or six wall widths was reached. (Figure 21.)

As might be logically expected, SPL from the model with the perforated walls conformed to the minus six db asymptote at a closer distance than for the solid walled model. There was too little data from the small scale models alone, however, to form any firm conclusions regarding the region where the farfield sound behavior begins.

Large Scale Model Results

Directivity Patterns

Immediately upon beginning the large scale model testing, even before making any actual measurements, the presence of the strong corner lobes was readily noted by ear. One could clearly hear a very marked increase in the sound level while walking past the corners of the models.

Subsequent measurement of these lobes yielded sound directivity patterns for the lower octave bands nearly identical to those of the small scale models, as can be seen in Figure 22. While

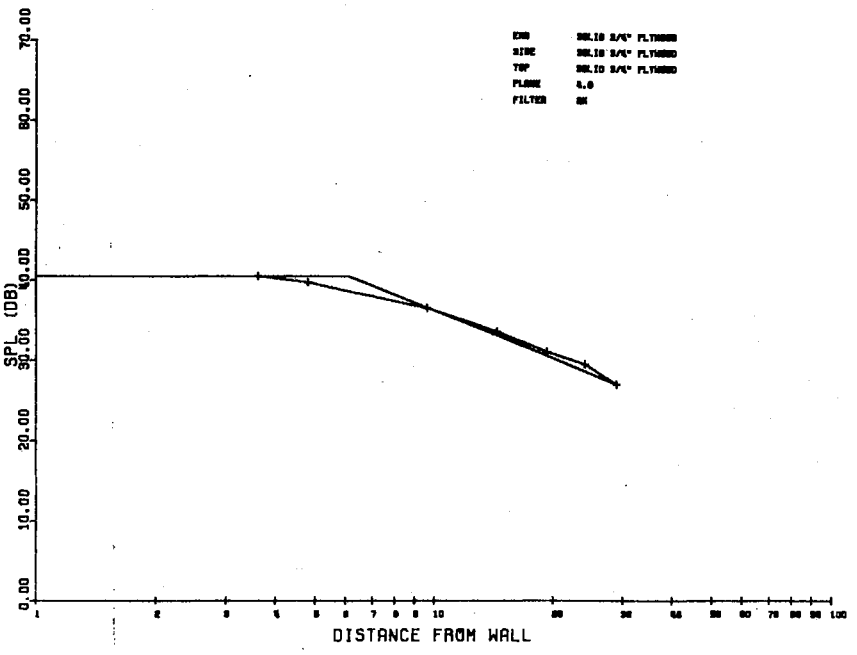

Figure 20. SPL Versus Distance Curve, Small Scale Model (2000 Hz with all Solid Walls)

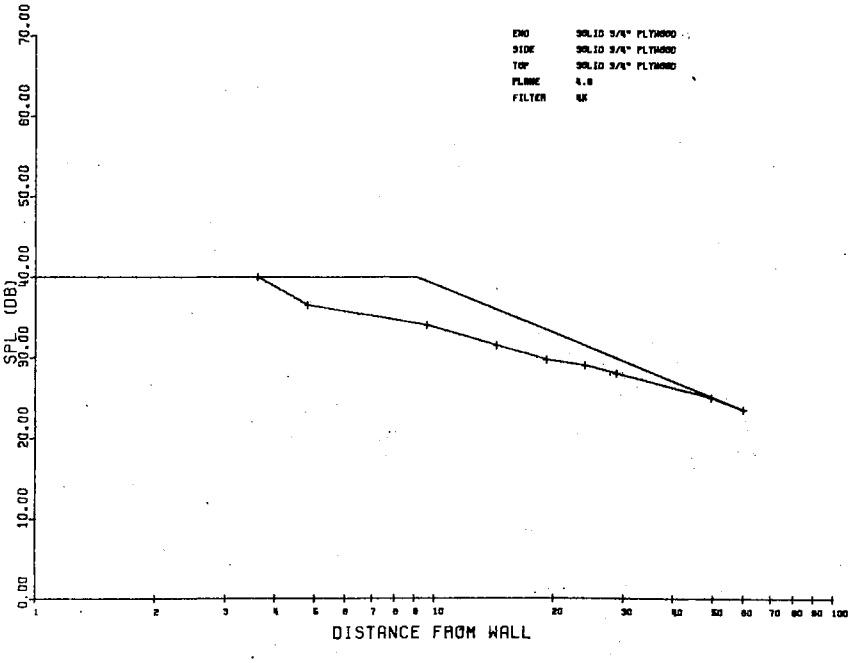

Figure 21. SPL Versus Distance Curve, Small Scale Model (4000 Hz with all Solid Walls)

comparing the directivity patterns in the preceding section on small scale models, one must consider the difference in scale size. Table I gives the comparison of the small scale versus large scale model frequencies.

TABLE I

COMPARISON OF MODEL FREQUENCIES

Small Scale Models (1/3 Octave)		Large Scale Models (Full Octave)	
Center Frequency	Frequency Limits (x 1/10)	Frequency Limits	Center Frequency
1000	88.5 – 111.5		
2000	177. – 223.		
4000	354. – 446.		
8000	708. – 892.		
		167. – 333.	250
		333. – 667.	500
		667. – 1333	1000

In brief, the 1/3 octave band at 2000 Hz in the small scale model tests is analagous to the 250 Hz octave band in the large scale model tests; the 4000 to 400 Hz and the 8000 to 1000 Hz, respectively.

It was then observed that as the higher octave bands were measured two corner lobes appeared and were even stronger than those in the lower bands. (Figure 26.)

The rest of the large scale models were tested in turn and had the same general radiation patterns as the first one in every case, the only change being a slight decrease in the SPL on the axis of the longer wall. Part of this decrease can be attributed to the fact that as the building length was increased, the grid points where the SPL measurements were taken were slightly farther away from the longer wall than the shorter wall. In the case of the 8 foot by 16.67 foot model, approximately 1 db decrease at a radius of 58 feet can be attributed to this 4 foot increase in distance.

The change in the radiation patterns with increasing model length is illustrated in Figures 22 through 25 for the 250 Hz octave band and in Figures 26 through 29 for the 4000 Hz octave band. The similarity of patterns for all source sizes within any given octave band held true throughout the experiments. The complete transition of the directivity pattern shapes with changing octave bands is illustrated in Figures 30 through 35 for the 8 foot by 12.67 foot model. Again this transition of the patterns for the particular case shown in these figures is typical of all the model lengths.

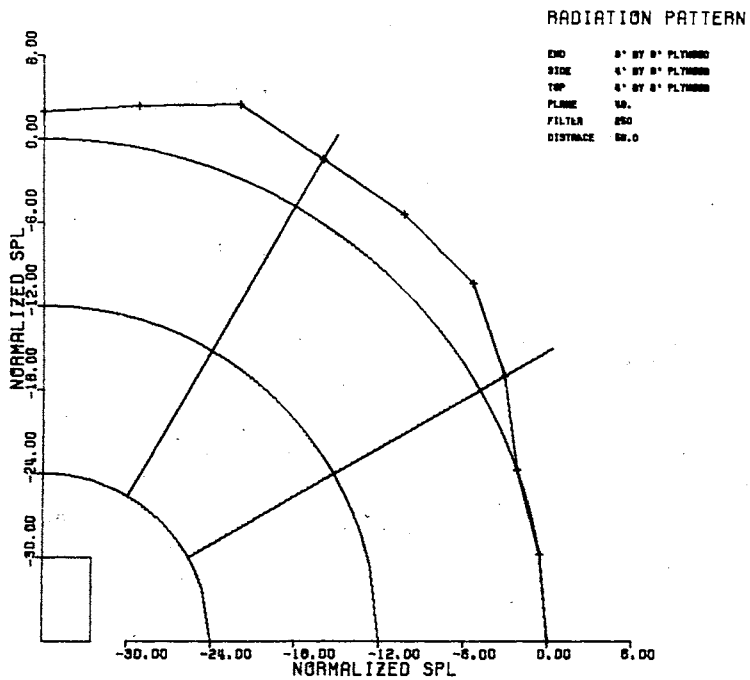

Figure 22. Directivity Pattern of Large Scale Model (250 Hz Octave Band, 8.' by 4.67')

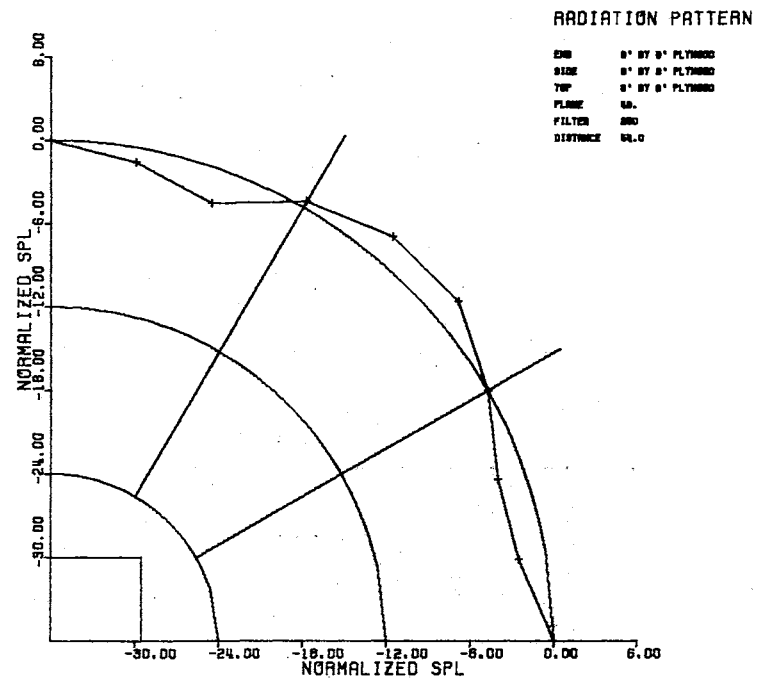

Figure 23. Directivity Pattern of Large Scale Model (250 Hz Octave Band, 8.' by 8.67')

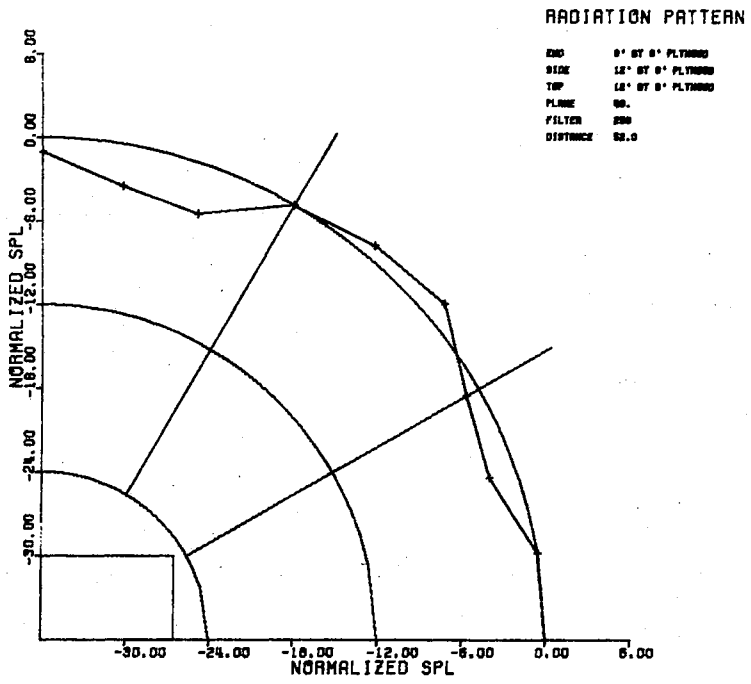

Figure 24. Directivity Pattern of Large Scale Model (250 Hz Octave Band, 8.' by 12.67')

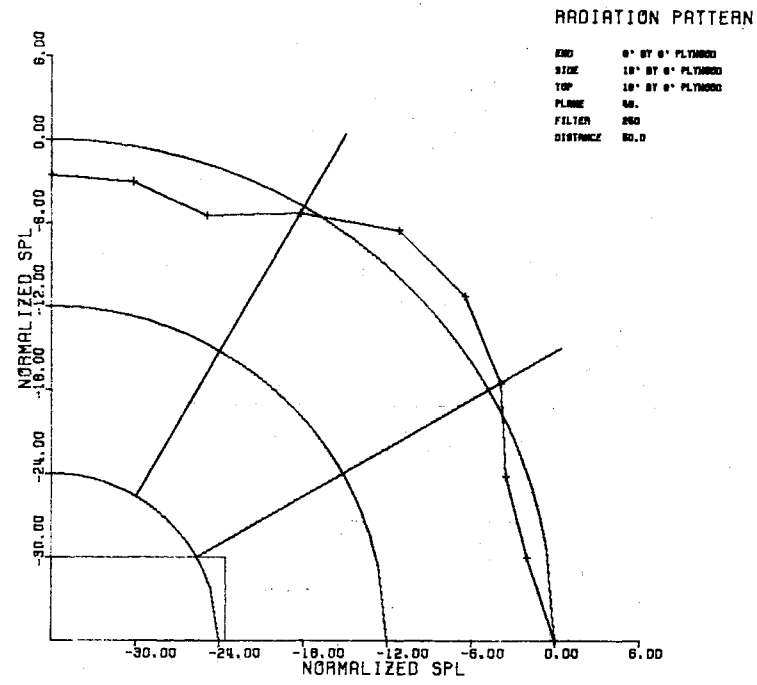

Figure 25. Directivity Pattern of Large Scale Model (250 Hz Octave Band, 8.' by 16.67')

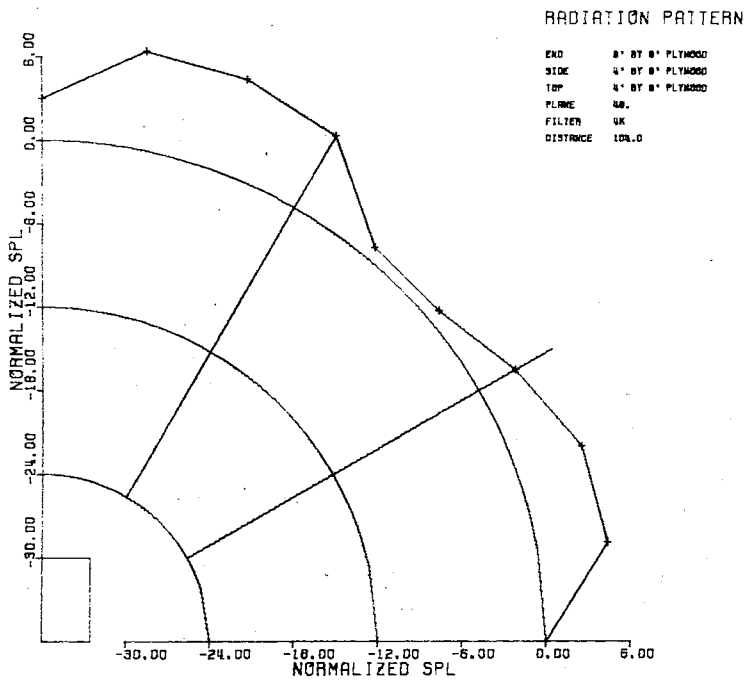

Figure 26. Directivity Pattern of Large Scale Model (4000 Hz Octave Band, 8.' by 4.67')

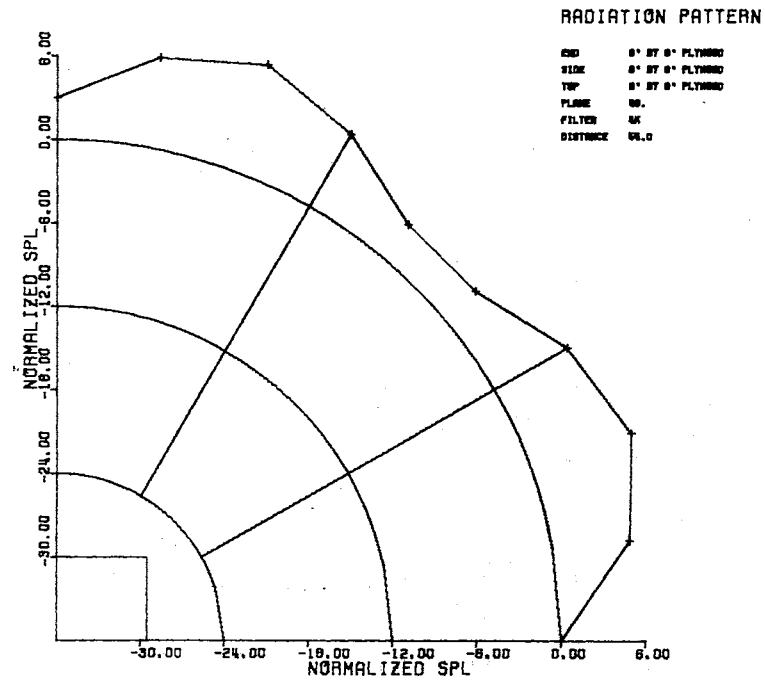

Figure 27. Directivity Pattern of Large Scale Model (4000 Hz Octave Band, 8.' by 8.67')

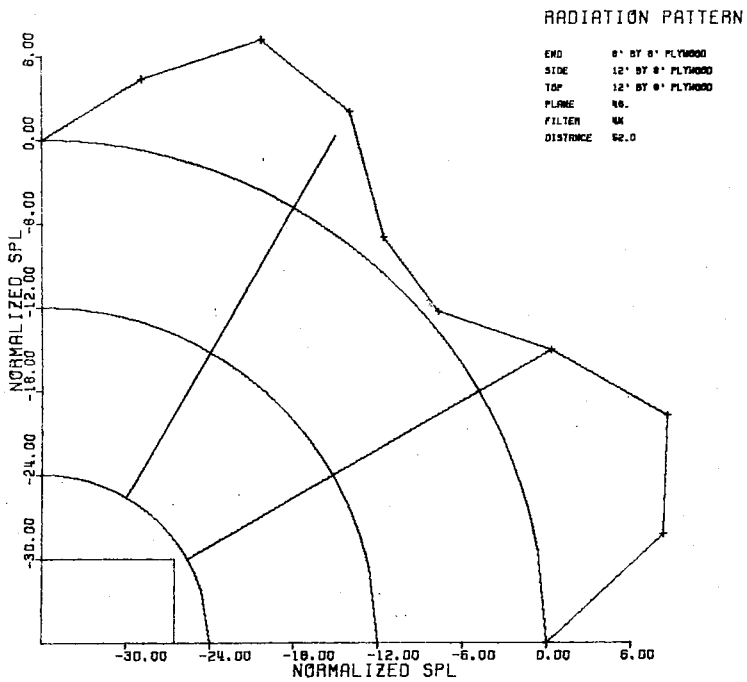

Figure 28. Directivity Pattern of Large Scale Model (4000 Hz Octave Band, 8.' by 12.67')

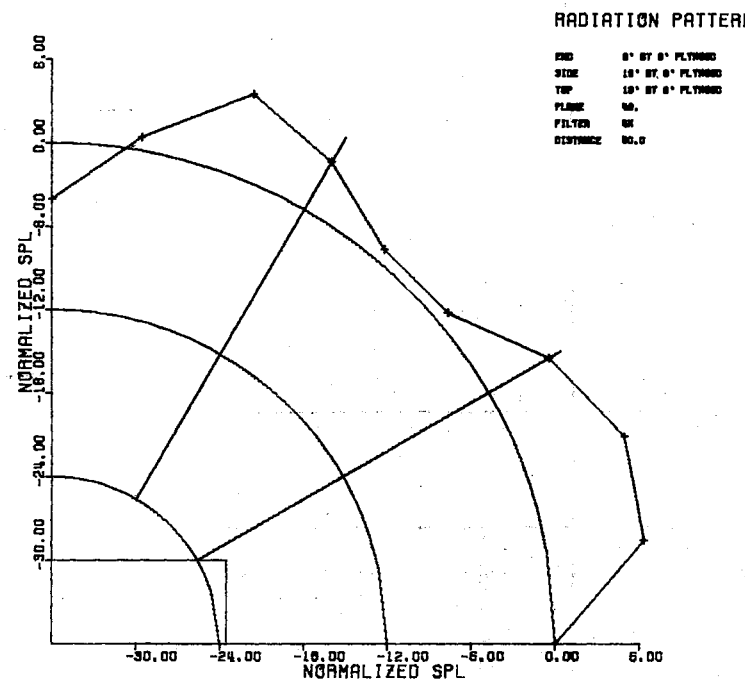

Figure 29. Directivity Pattern of Large Scale Model (4000 Hz Octave Band, 8.' by 16.67')

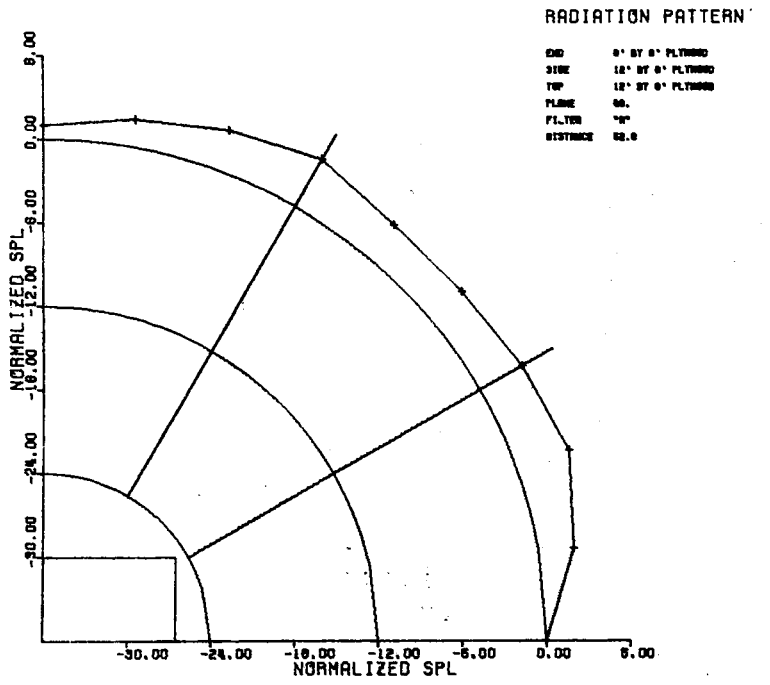

Figure 30. Directivity Pattern of Large Scale Model (A Weighted 8.' by 12.67')

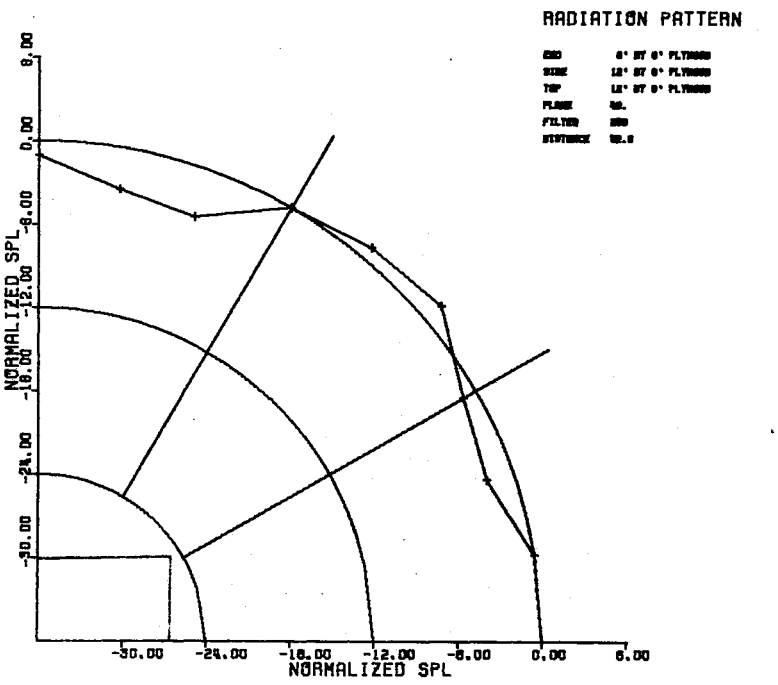

Figure 31. Directivity Pattern of Large Scale Model (250 Hz Octave Band, 8.' by 12.67')

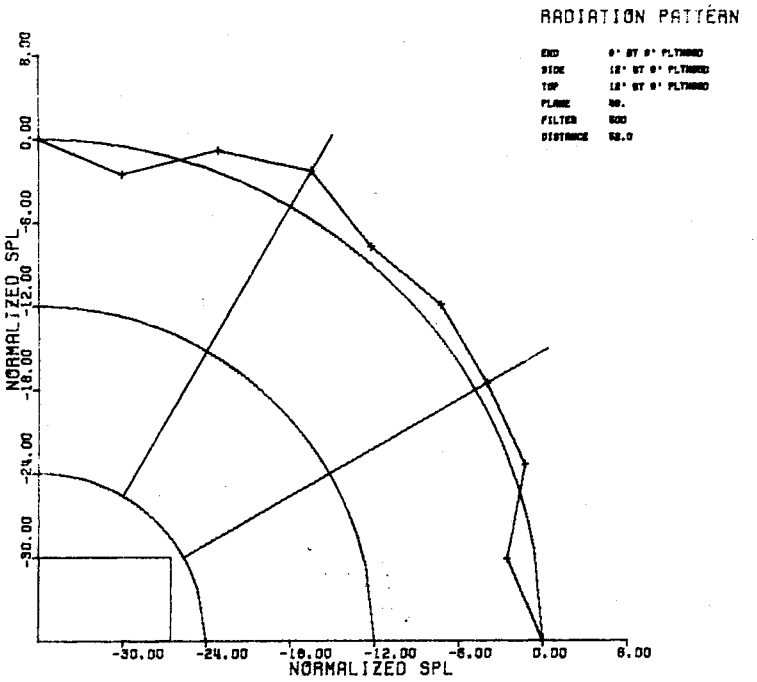

Figure 32. Directivity Pattern of Large Scale Model (500 Hz Octave Band, 8.' by 12.67')

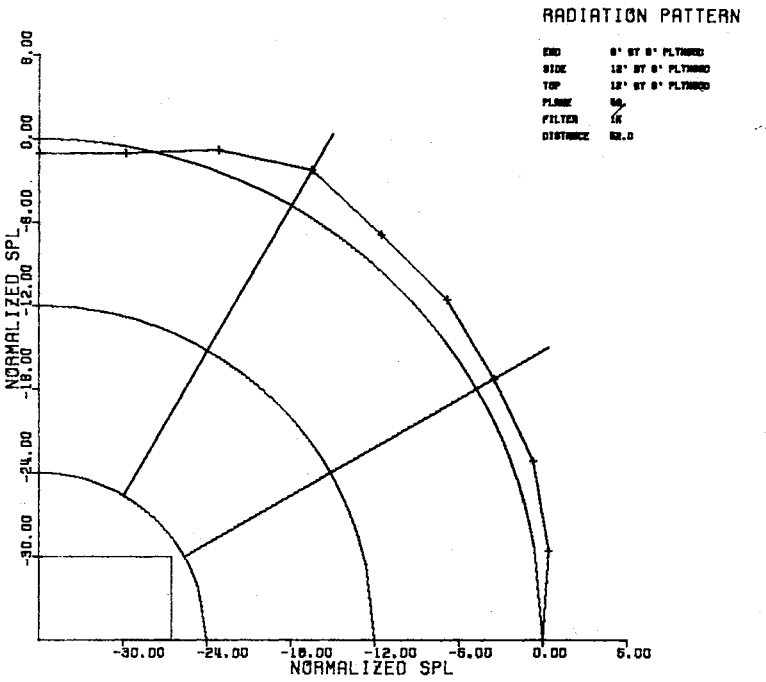

Figure 33. Directivity Pattern of Large Scale Model (1000 Hz Octave Band, 8.' by 12.67')

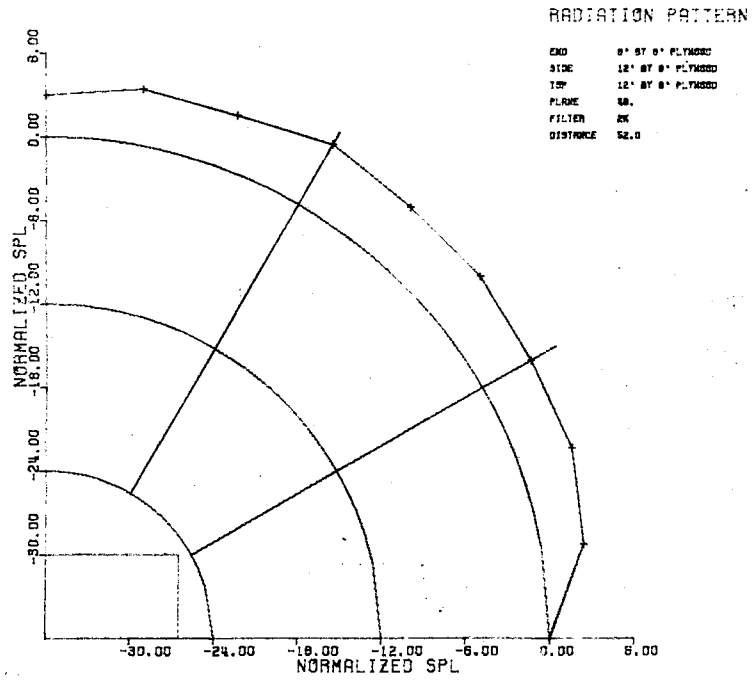

Figure 34. Directivity Pattern of Large Scale Model (2000 Hz Octave Band, 8.' by 12.67')

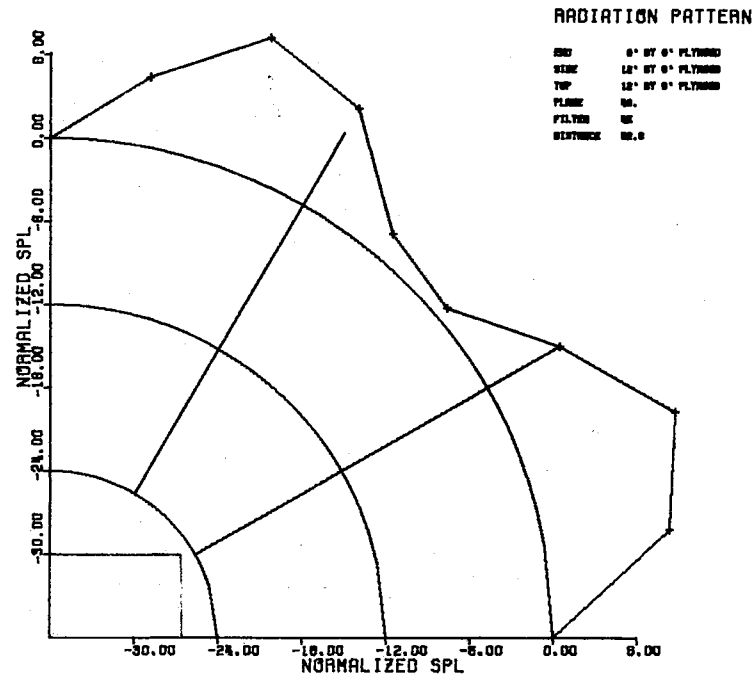

Figure 35. Directivity Pattern of Large Scale Model (4000 Hz Octave Band, 8.' by 12.67')

SPL Decrease With Distance

As with the small scale models, it was found that the variation of SPL with distance was not quite as well behaved as the inverse distance squared law suggested especially in the region that might be called the near farfield. In the lower octave band the plots again appeared to approach the minus six db asymptote at a closer distance than in the higher octave bands. The anamalous excess atmospheric attenuation of mid-range frequencies between about 300 and 600 Hz reported by other authors (9, 10) was very evident in all of the plots of SPL versus distance for the 250 and 500 Hz octave bands. It was unusual only in that it was evident at such close distances. Figure 36 and 37 are frequency spectrums at three inches, and at six feet from the surface of the models and also illustrates this attenuation. Data reported by these authors (9, 10, 11, 12) indicated that all other excess attenuation was negligible in this study. Weiner and Keast (10) developed idealized attenuation functions for both upwind and downwind sound propagation (less molecular absorption) which did not give any excess attenuation at distances less than 250 feet upwind or less than 500 feet downwind. Using an example of 50 percent relative humidity and 25 degrees centigrade, Harris's (12) results under laboratory conditions gave sound absorption in air ranging from .1 db per 100 meters at 250 Hz to 2.5 db per 100 meters at 4000 Hz. This was less than 1 db attenuation per 100 feet, and in this study 150 feet

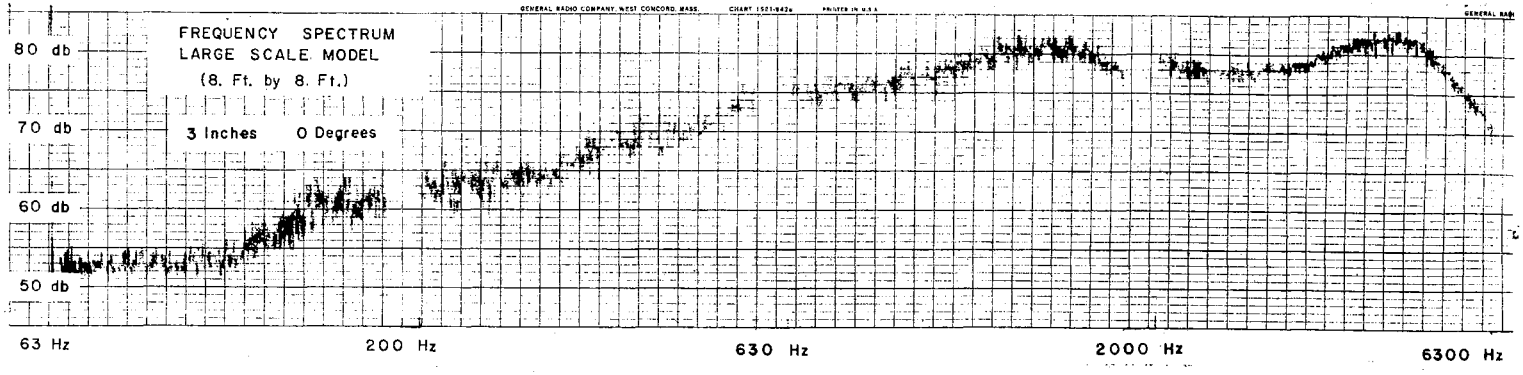

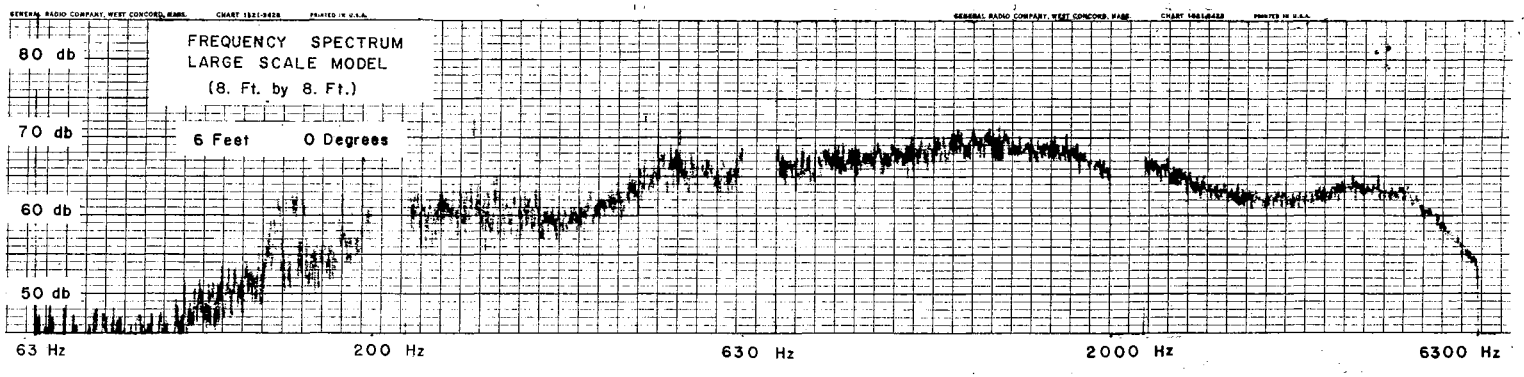

Figure 36. Frequency Spectrum of the 8' by 8' Large Scale Model (0^{o})

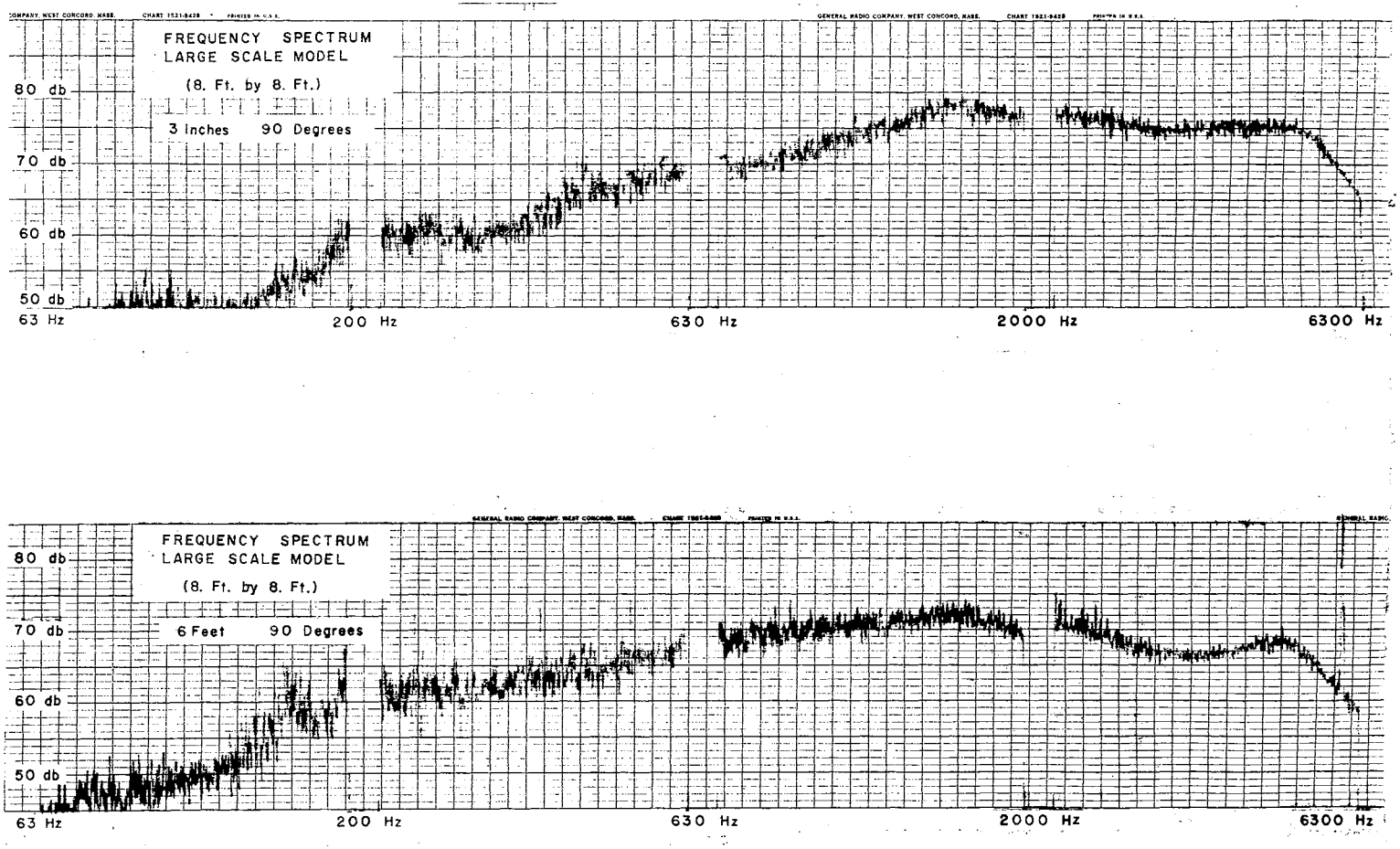

Figure 37. Frequency Spectrum of the 8' by 8' Large Scale Model (90^{o})

was the maximum distance where measurements were taken. Wind and temperature gradients cause the well known "shadow zones" but not at such close distances as in this study. Regardless, as previously stated, measurements were taken in the early morning hours on calm days to minimize wind and temperature gradients. Other authors results similarly gave maximum values of total excess attenuation of 1 to 2 db per 100 feet at 4000 Hz (the most severe case). (11, 16) The variation in behavior of SPL with distance through the frequency bands can be seen in Figures 38 and 39.

It was concluded from study of all the SPL versus distance plots that, for the inverse square law to be completely valid at high frequencies the SPL must be plotted with respect to the distance from an "image" source at some point within the model, and not the wall itself. This can be deduced logically since the added dimension of depth of the model would obviously add depth to the sound source also.

That this image source forced the SPL to fit the minus six db asymptote closer can be seen by adding half the model length, four feet, to all the distances plotted in Figure 39. Four feet is quite significant at close distances but less significant at greater distances. At the lower frequencies, however, the actual source appeared to be the wall surface itself, as the SPL curve fit the asymptote quite closely.

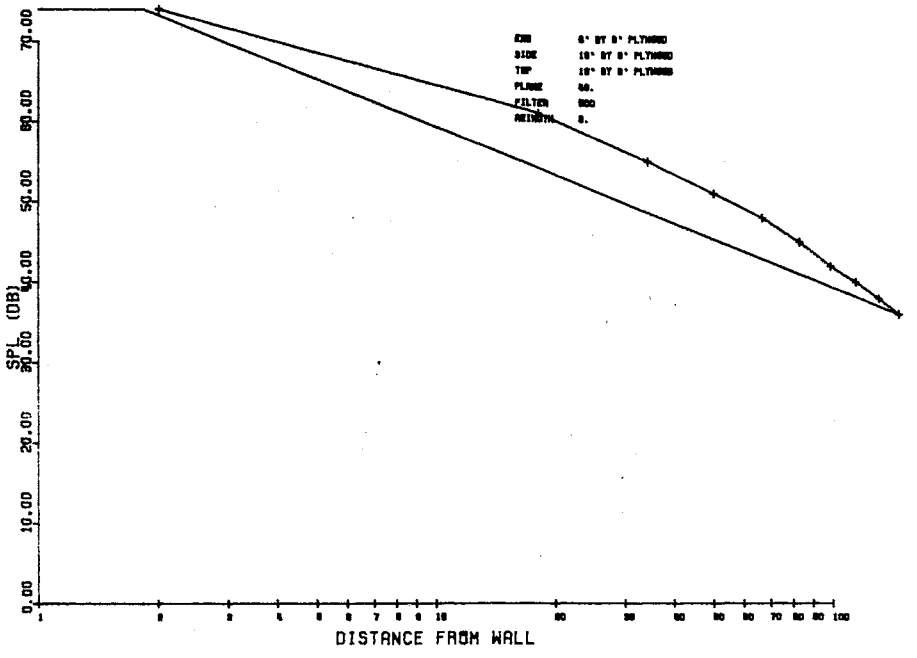

Figure 38. SPL Versus Distance Curve, Large Scale Model (500 Hz Octave Band, 8.' by 12.67')

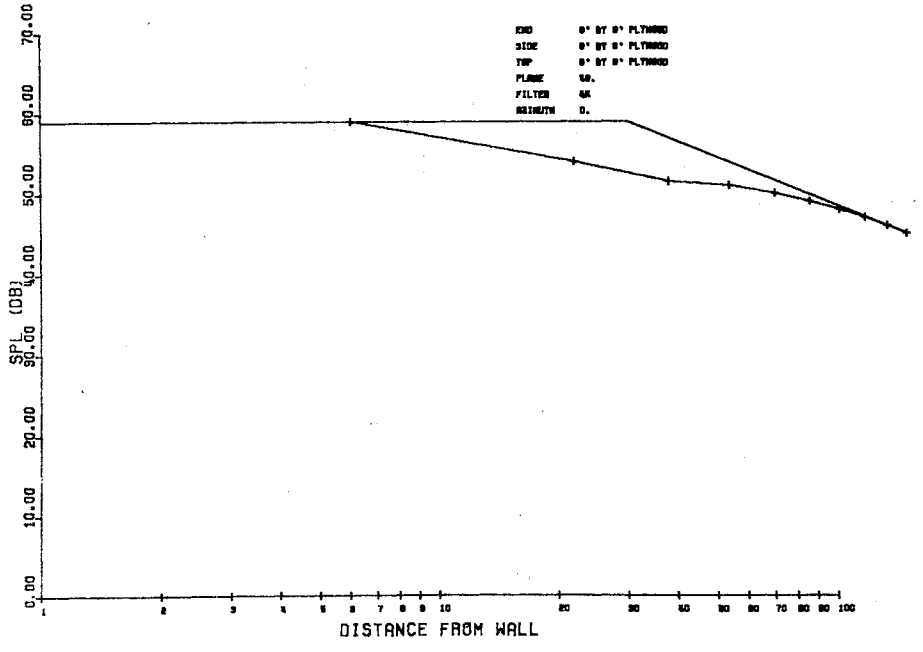

Figure 39. SPL Versus Distance Curve, Large Scale Model (4000 Hz Octave Band 8.' by 8.67')

Water Table Results

The experiments with the water table were conducted so the directivity patterns could be visually studied since surface waves on a water table provide a graphical representation of wave motion not available by any other method. In such a study the amplitude of a water surface wave is analagous to the pressure of an acoustic wave in air.

It was necessary to keep the source dimension to wave length ratios (d/λ) approximately the same as for the acoustic models. The actual range of d/λ ratios was from less than 1 to 60, but the range of greatest interest was between 7 and 28. These values of d/λ dictated a surface wave frequency range of approximately 30 to 120 Hz. Details of how this frequency range was determined is contained in the appendix. The membrane and oval loudspeaker drivers were both capable of generating frequencies over this range.

Corner lobes were observed being radiated from both of these drivers at several frequencies throughout the range of interest, but there were also several frequencies where the generators appeared to vibrate in phase and plane waves were generated which created no corner lobes. Figures 40 through 43 are photographs showing details of the wave patterns generated. The significance of this data is that at frequencies when the source wall acts as "multiple sources" this strong reinforcement at the corners occurs, and it is

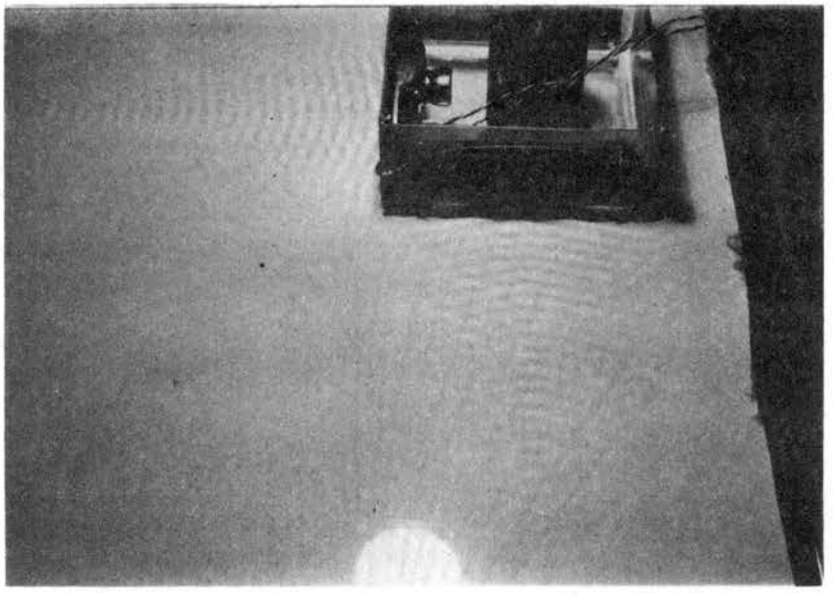

Figure 40. Water Table Oval Loudspeaker Driver (26 Hz)

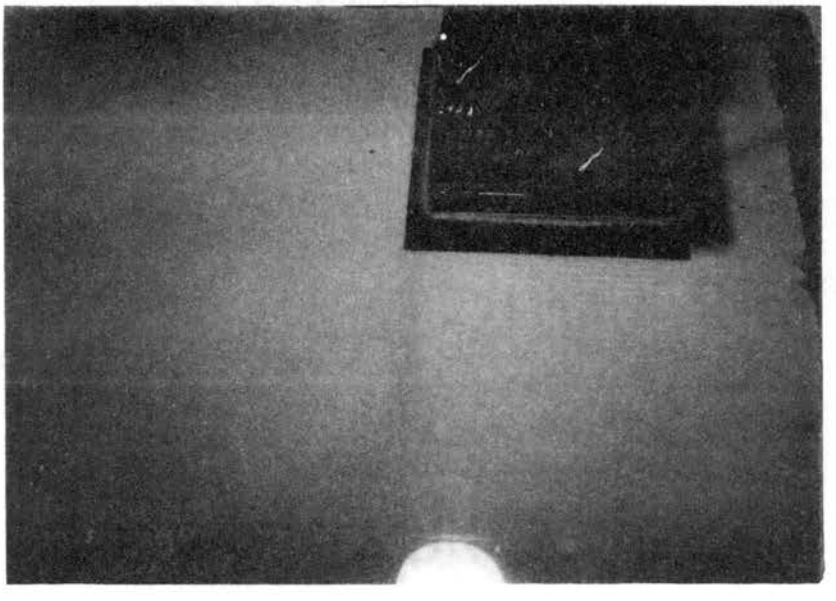

Figure 41. Water Table Membrance Driver (110 Hz)

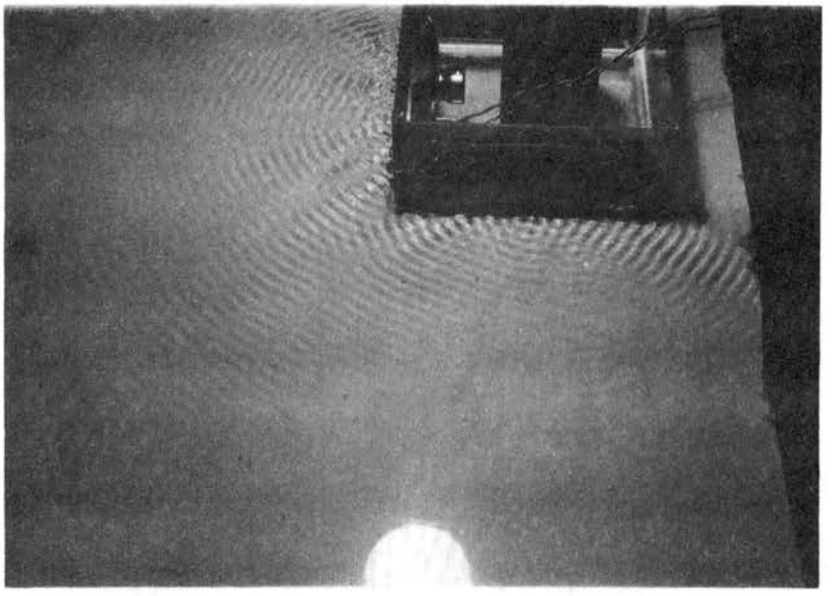

Figure 42. Water Table Oval Loudspeaker Driver (68 Hz)

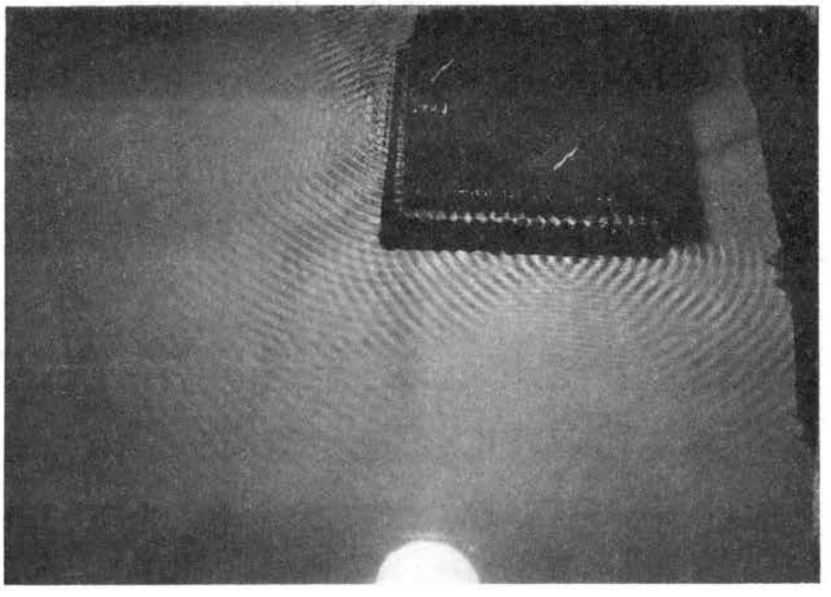

Figure 43. Water Table Membrane Driver (138 Hz)

logically assumed that there are many such frequencies throughout each octave band. The fact that this strong corner reinforcement occurred with both driver designs was further evidence that radiation is more strongly dependent on geometry than on wall dynamics.

Attempts at actual measurement of the amplitude of the gravity waves generated were fruitless, primarily because of their small amplitude. Briefly, the methods attempted and the difficulties encountered with each are summarized next.

First, a fine (.1 inch) square grid on clear acetate was immersed vertically in the water so a photograph of the wave from the side would show the amplitude directly in the picture. The surface tension of the water was sufficiently high and the wave amplitude so low that all wave motion stopped adjacent to the grid. Then an attempt was made to mount a needle point on a micrometer type carrier and lower it just until contact was observed and thus measure the amplitude from the surface of the undisturbed water surface to the wave crest. This also was prevented by the surface tension and small wave amplitude.

Stereoscopic photography was used but was also unsuccessful because of unavailability of a camera with widely separated lens, and a good interpreter. Lack of a suitable reference point on the water surface made accurate measurement by this method questionable at best.

The final method attempted was use of a Moire' grid. The untreated water surface did not afford enough reflection and neither the addition of white coloring nor aluminum dust on the surface helped significantly. In addition, the close proximity that the grid had to be located to the water surface to achieve the interference patterns made this method impractical. In short, the fringes could not be attained even with a grid of 64 lines-per-inch, and theory indicated 200 lines-per-inch were necessary for sufficient accuracy.

Certainly measurement of the wave amplitudes was not impossible, but insufficient time plus limited value of the results prompted the decision to abandon further attempts.

Summary of Experimental Results

Spherical Spreading

The results of all the data gathered during this research indicated that spherical spreading did not occur at some point a given number of wall widths away as simply as suggested in some of the current literature. Examination of Figure 39, for example, illustrates that if spherical spreading were assumed to exist at three wall widths away, an error of over seven db would be introduced at distances of 100 feet or more. In fact spherical spreading did not begin until approximately ten wall widths away.

It was determined, however, that the data was reasonably consistent for all large scale models within any frequency band when the distances were normalized with the cube root of the product of the three major dimensions (i.e. the volume).

$$d = \sqrt[3]{\text{width}*\text{length}*\text{height}}$$

A characteristic distance was defined as that distance from the wall to the point where the minus six db asymptote intersects the value of the intensity at the wall surface. The distance from the wall itself was chosen because of the uncertainty of the additional distance to the image source discussed earlier. This characteristic distance was then related to the octave bands as shown in Table II. Though there was not a large quantity of data for a statistical analysis, it was felt that the results were consistent enough to be the basis of a good design guide. It was assumed that any design guide should be conservative, within reason, and that neither the "average" nor the "worse case" figures were the best to use. Therefore, the weighted figures in the third column are recommended for use. These figures are plotted in the curve shown in Figure 44. Also shown in Figure 44 are the data points from the corresponding small scale model tests.

Uncorrected data on the noise measurements from the new steel building were generally well below this curve in Figure 44, however, when considered as a very large 7.5/1 scale model and the actual

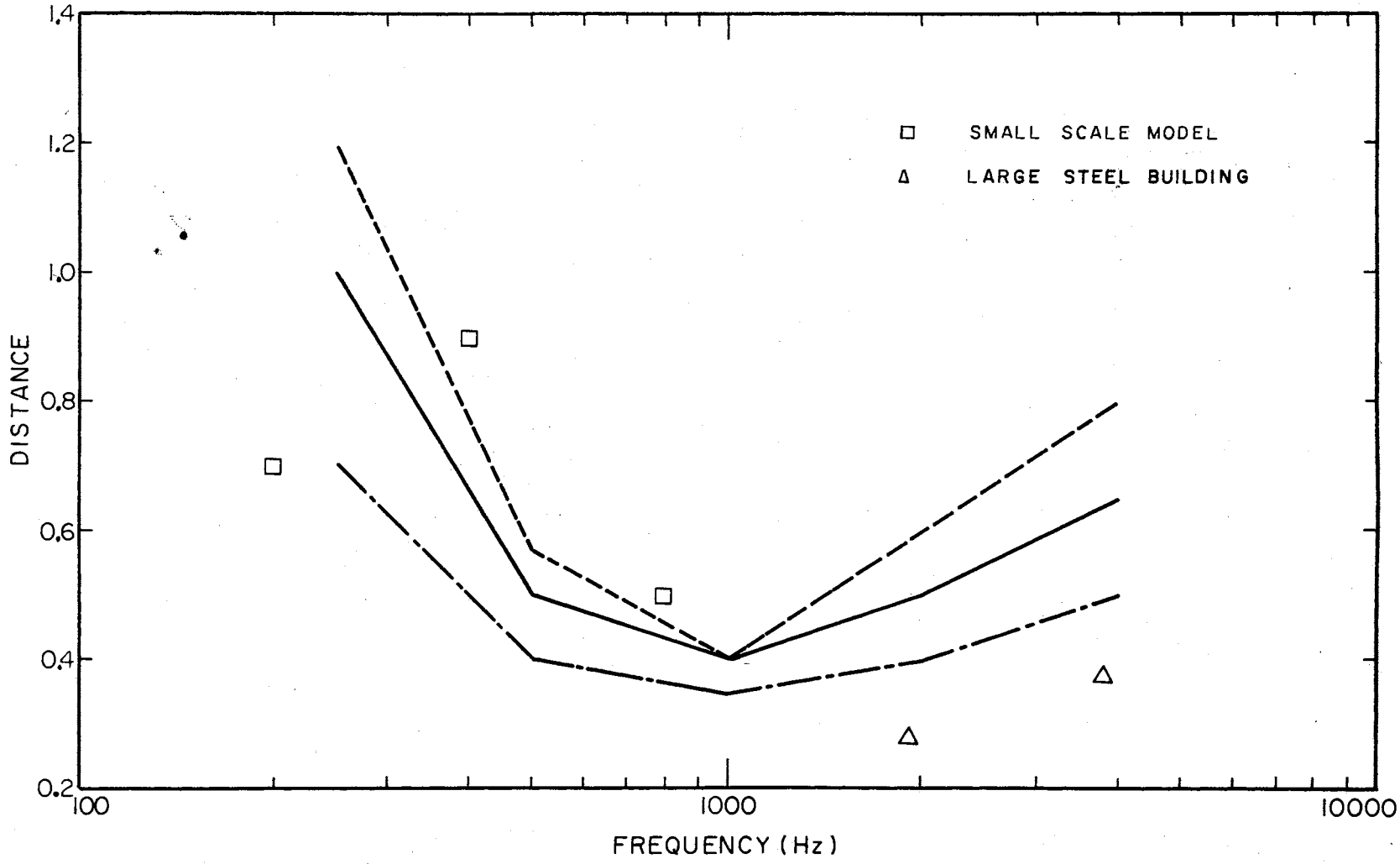

Figure 44. Characteristic Distance Versus Frequency

frequencies adjusted upward accordingly, the data fit much closer as seen by the two data points on the curve.

TABLE II

STATISTICAL DATA SPL VERSUS NORMALIZED DISTANCE CURVES

	Average		Worst		Skew	
Octave Band	0 db	-6 db	0 db	-6 db	0 db	-6 db
0	.4	.45	.6	.7	.5	.65
250	.7	.9	1.2	1.6	1.0	1.7
500	.4	.6	.55	1.0	.5	.8
1000	.35	.5	.4	.8	.4	.6
2000	.4	.3	.6	.6	.5	.4
4000	.5	.1	.8	.4	.65	.2

To assist in making a better estimated plot of the SPL farfield behavior, the points at which the measured SPL had decreased 6 db from the surface intensity were related statistically to the same dimensionless distance used previously. These results are also given in Table II and plotted in Figure 45.

Given then the fact that one knows the dimensions of a structure under consideration, and an estimate of the sound intensity at the outside surface, use of the curves in Figures 44 and 45 will give a very

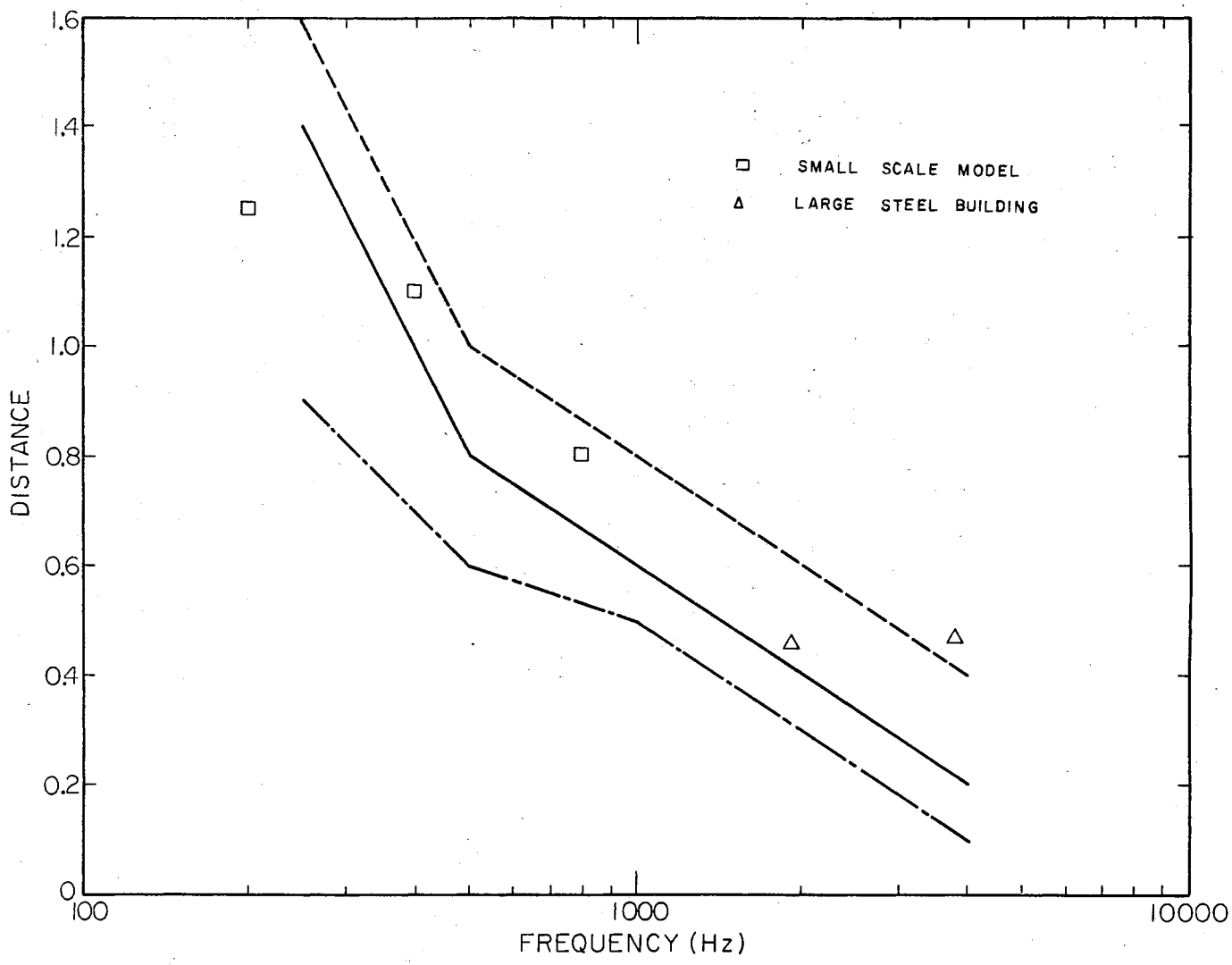

Figure 45. Distance to 6 db Down Point Versus Frequency

good estimate of the SPL decrease with distance. Application of Figure 44 locates the asymptote and Figure 45 the location of the first 6 db decrease, and these two known points aid in sketching the approximate curve.

Directivity Patterns

Examination of the data gathered during this research indicated very definitely that there was a strong relationship between geometry and radiation patterns. It was apparent very early in the project that the simple combination of two radiation patterns as shown in Figure 16 positioned on adjacent sides of a model would not yield the same radiation pattern as shown in Figure 18.

The most significant change in the radiation patterns with the increasing size of the large scale model was the slight shift in the positions of the lobes toward the axis of the narrower side. Further analysis indicated that the radiation patterns of the 12 and 16 foot long models could be approximated with the data from the 8 foot model, if corrections for geometry were made. This method of approximation merely analyzed the longer models as if they were two telescoping eight foot models expanded to the same total length. This procedure provided an estimate of the SPL to within approximately ten degrees of the axis of the longer side. The geometrical relationship between the two telescoping equilateral sources expanded to a length of 12

feet is shown in Figure 51. As shown graphically in the figure, any given point in space is at a different angle from the center of the equilateral source than from the center of whole source, and also at a different distance. Calculation of this ΔR is a simple matter and varies approximately linearly with the angle.

The data for the eight foot (cubed) large scale model was then smoothed and resulted in the "standard equilateral source" directivity data given in Table III. This data is also plotted in Figures 46 through 50. This directivity data can now be used in conjunction with the SPL distance curve from the preceding section to approximate the sound intensity around a structure by adding the db correction in Table III to the estimate of the on-axis SPL. Note that this will not be a true radiation pattern, because it will not be centered on the center of the structure; however, one can be constructed with geometrical corrections for angle and distance changes.

To estimate a directivity pattern at 58 feet in the example in Figure 51 for a sound source with predominant 1000 Hz octave band components, the first step would be to determine all the angles (θ_i) from the center of the equilateral source to the points at every ten degrees on the 58 foot arc around the center of the source. Once this is determined, the changes in SPL for each of these angles can be read from the curve in Figure 48. The error in these db corrections due to the change in distance, ΔR, can be found from the plot of

TABLE III

SMOOTHED DATA FOR EQUILATERAL SOURCE
(Correction in Db)

Octave Band	Angle (Degrees)									
	0	10	20	30	40	50	60	70	80	90
250	0	-2	-2	0	3	3	0	-2	-2	0
500	0	1	2	3	4	4	3	2	1	0
1000	0	1	2	3	3	3	3	2	1	0
2000	0	2	5	4	3	3	4	5	2	0
4000	0	5	9	9	3	3	9	9	5	0

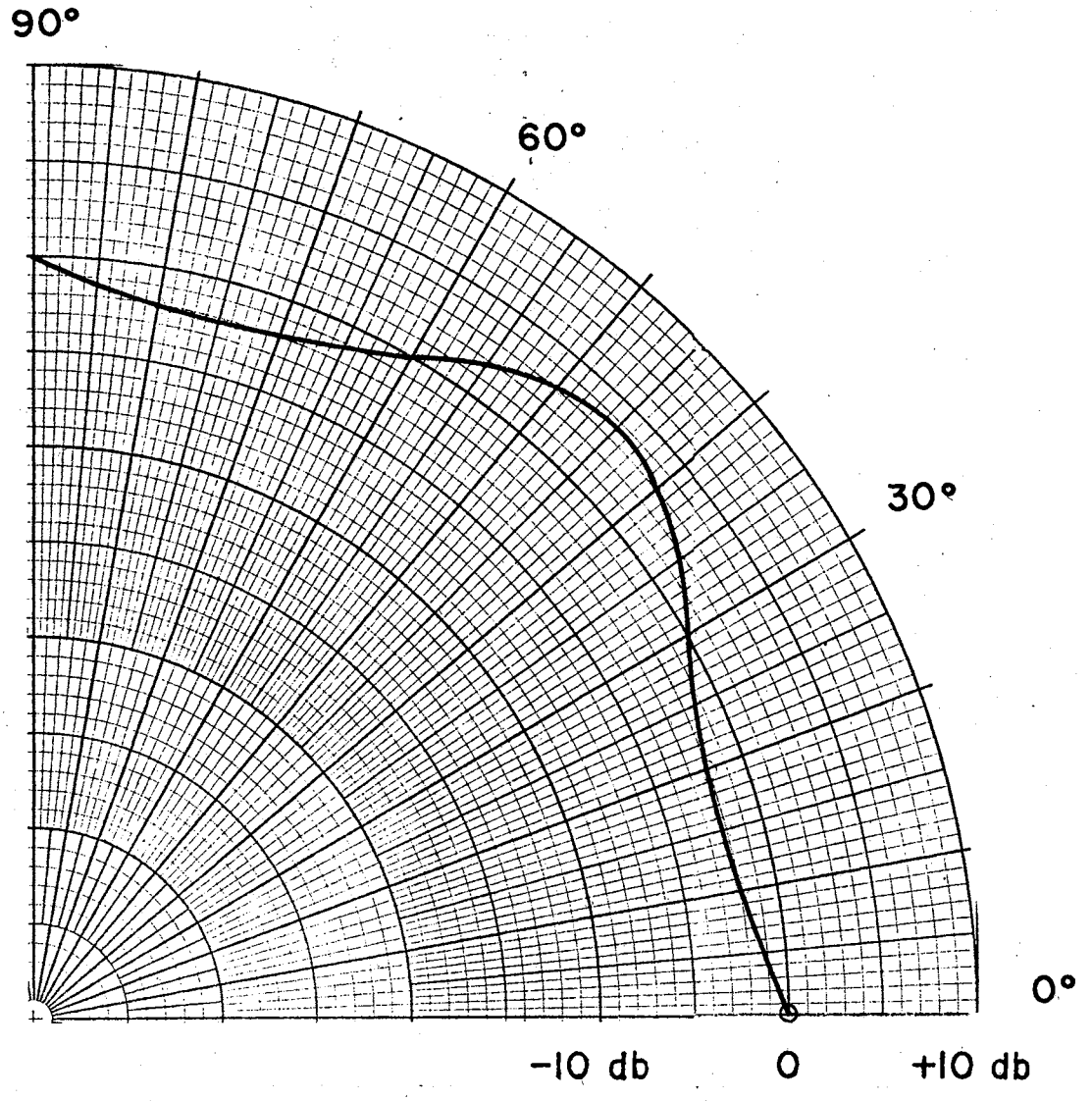

Figure 46. Smoothed Equilateral Source Directivity Pattern--250 Hz

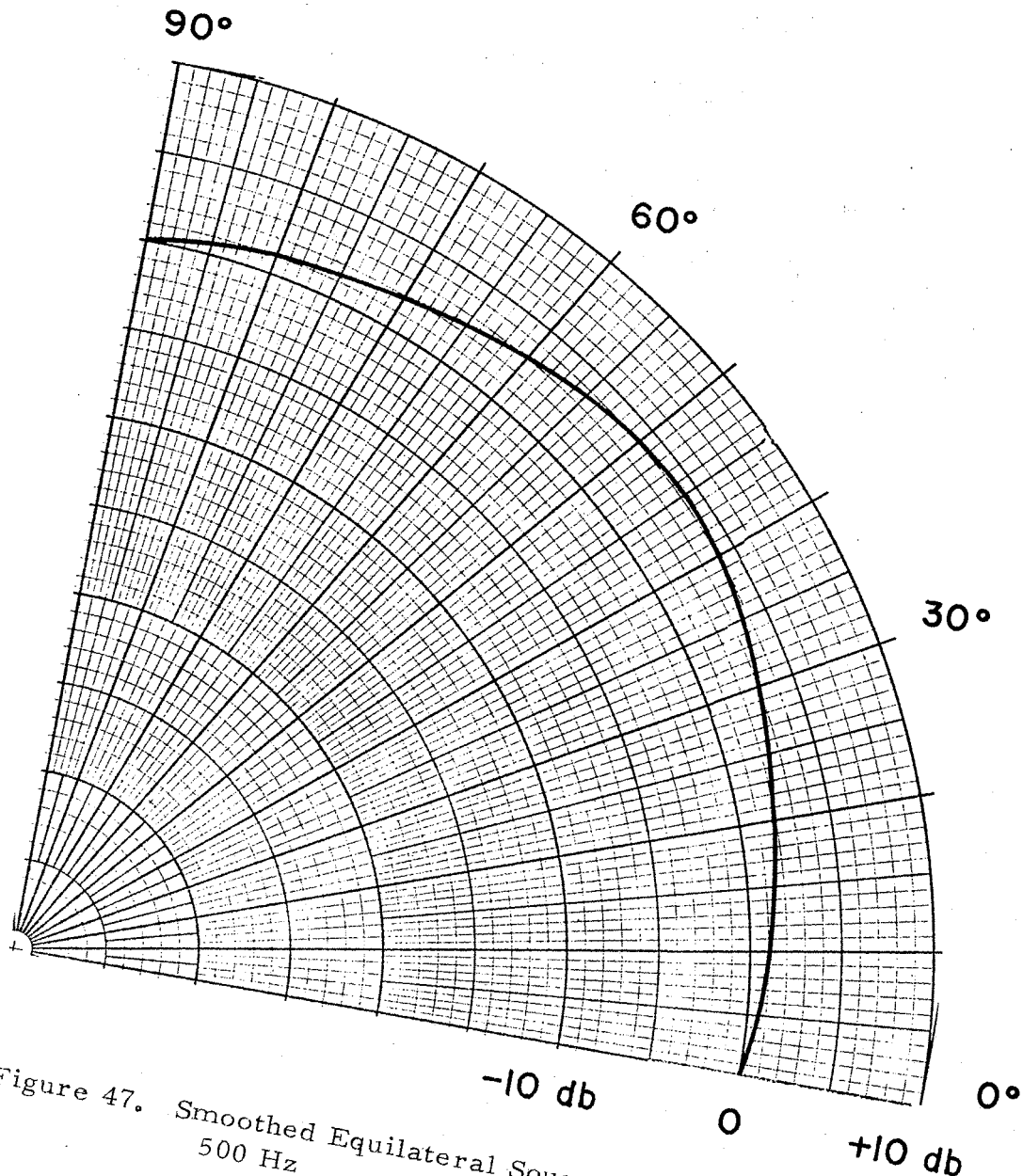

Figure 47. Smoothed Equilateral Source Directivity Pattern--
500 Hz

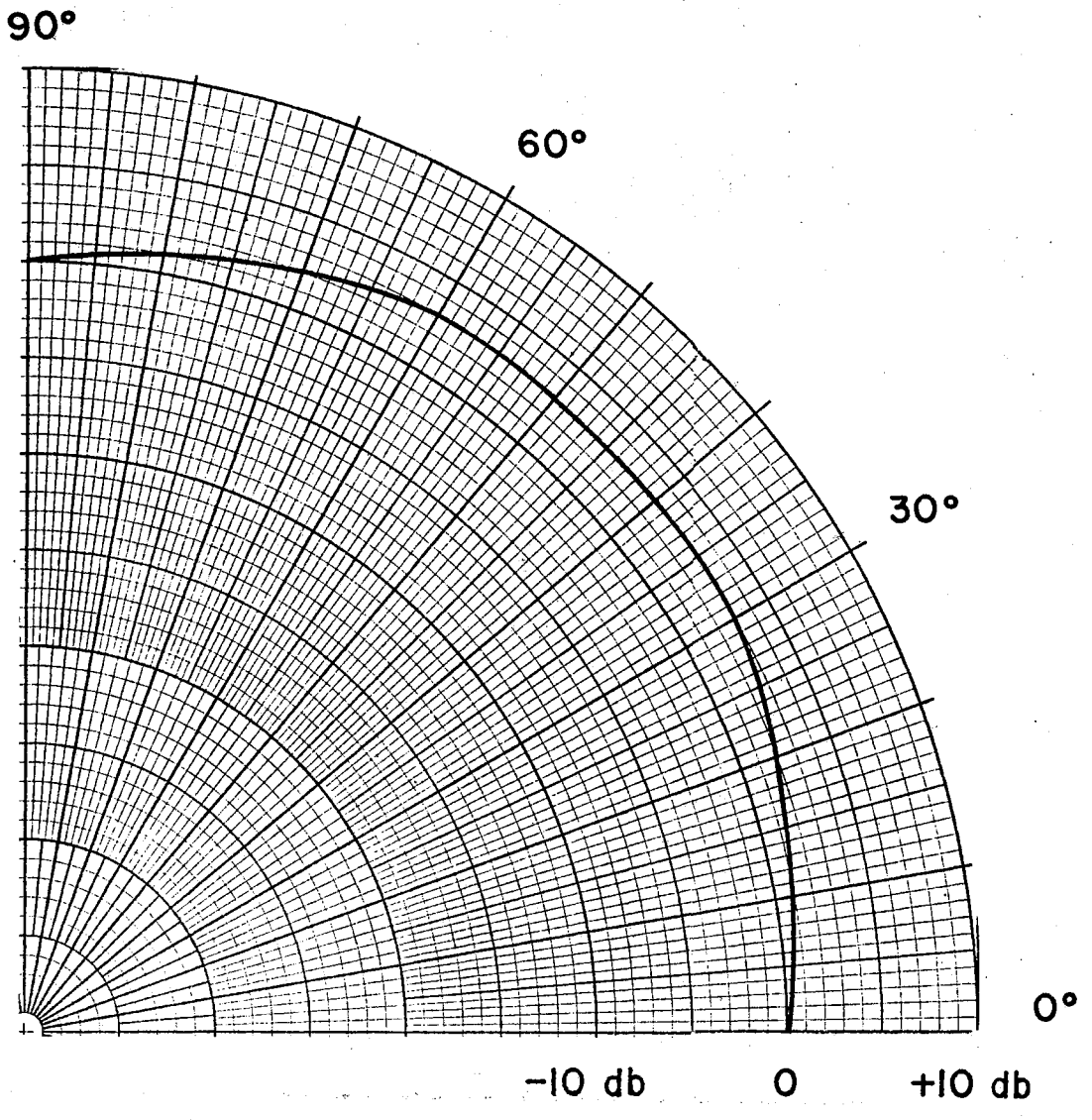

Figure 48. Smoothed Equilateral Source Directivity Pattern--1000 Hz

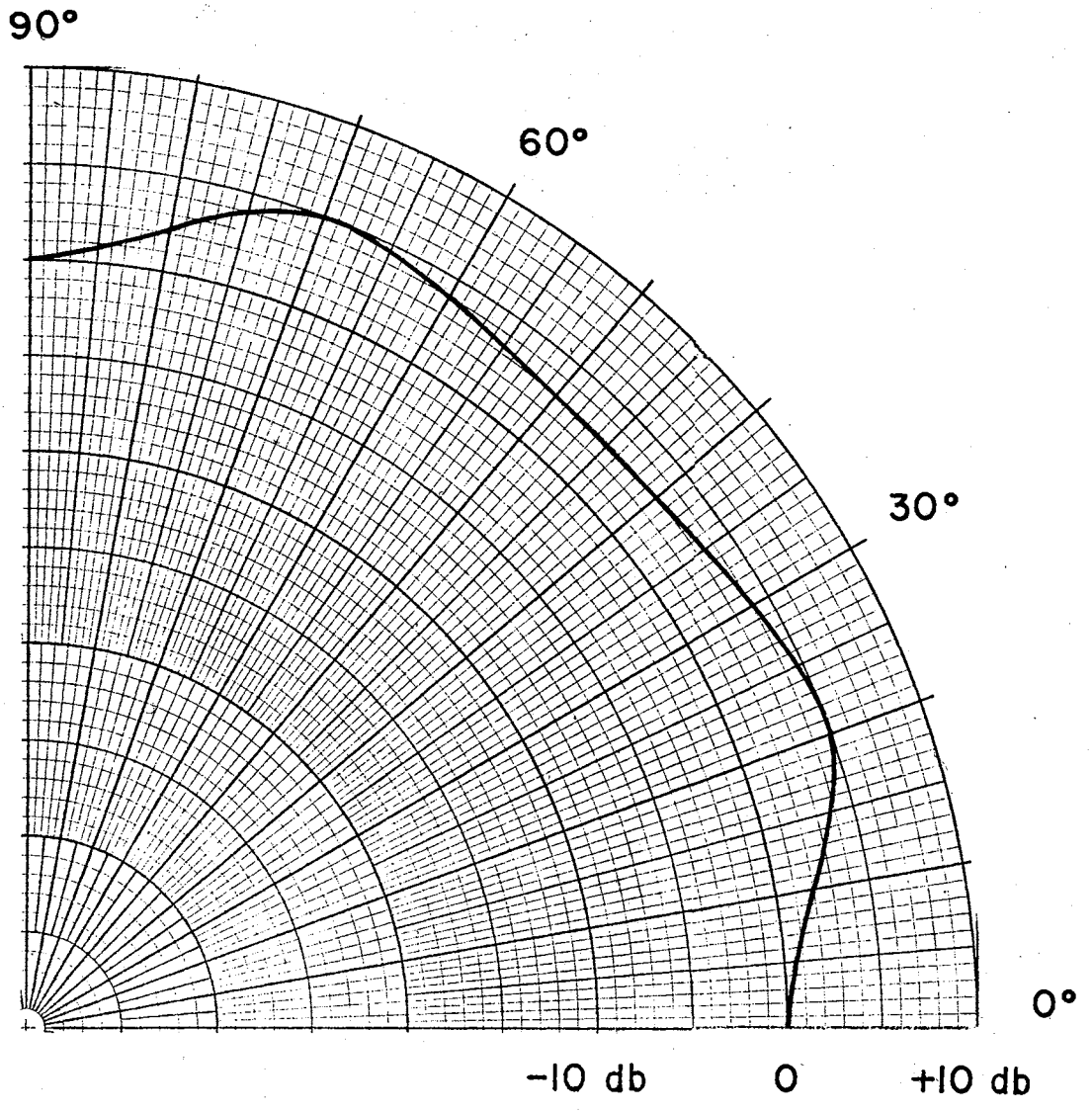

Figure 49. Smoothed Equilateral Source Directivity Pattern--
2000 Hz

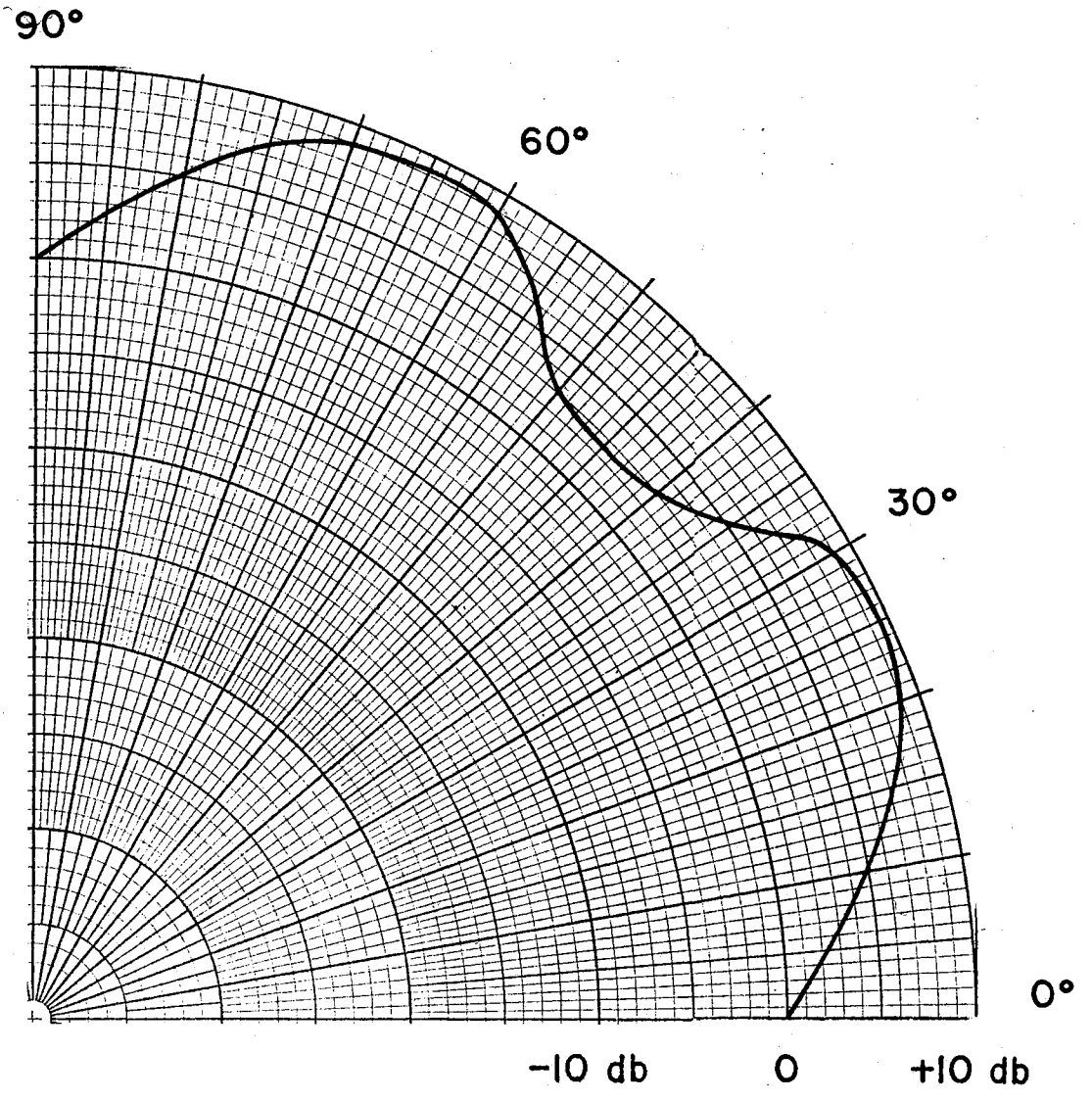

Figure 50. Smoothed Equilateral Source Directivity Pattern--4000 Hz

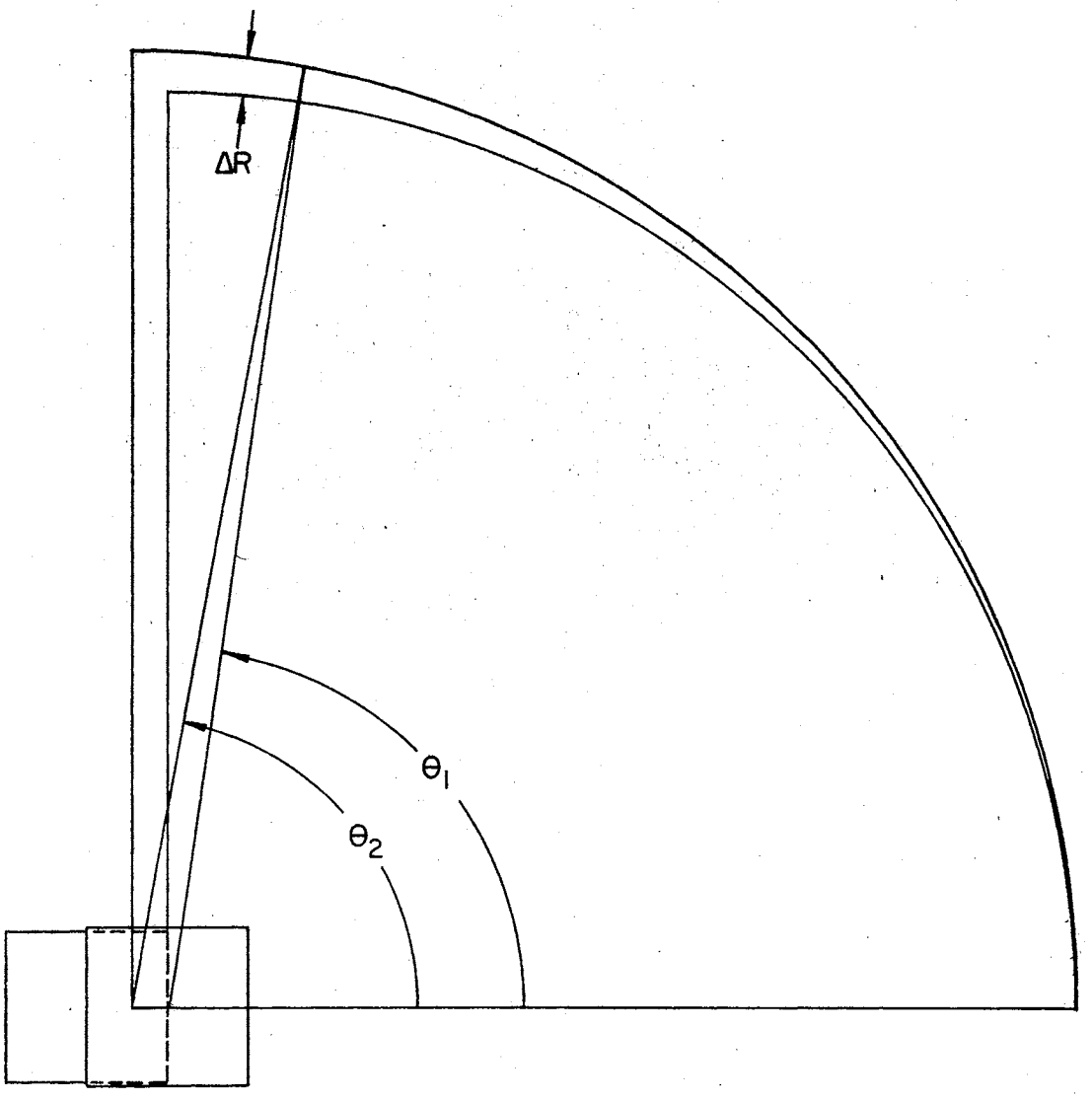

Figure 51. Geometrical Corrections for Telescoping Equilateral Source

SPL decrease with distance. The maximum error is at 90 degrees where ΔR is a maximum, two feet in this example. The change in SPL at 52 feet (from the wall) due to a two foot decrease in distance is less than one db, so no corrections need be made for ΔR, and the estimate will just be slightly more conservative. Plotting these changes in SPL at each point completes the directivity pattern from 0 to 80 degrees, and assuming the SPL constant from 80 to 90 degrees completes the quarter circle. The resulting estimate is shown in Figure 52 superimposed on the measured directivity pattern. Actual measured directivity patterns were approximated generally within one or two db by this method. The data in Table III is valid for dimensionless distances (page 57) between approximately three and six from the structure wall.

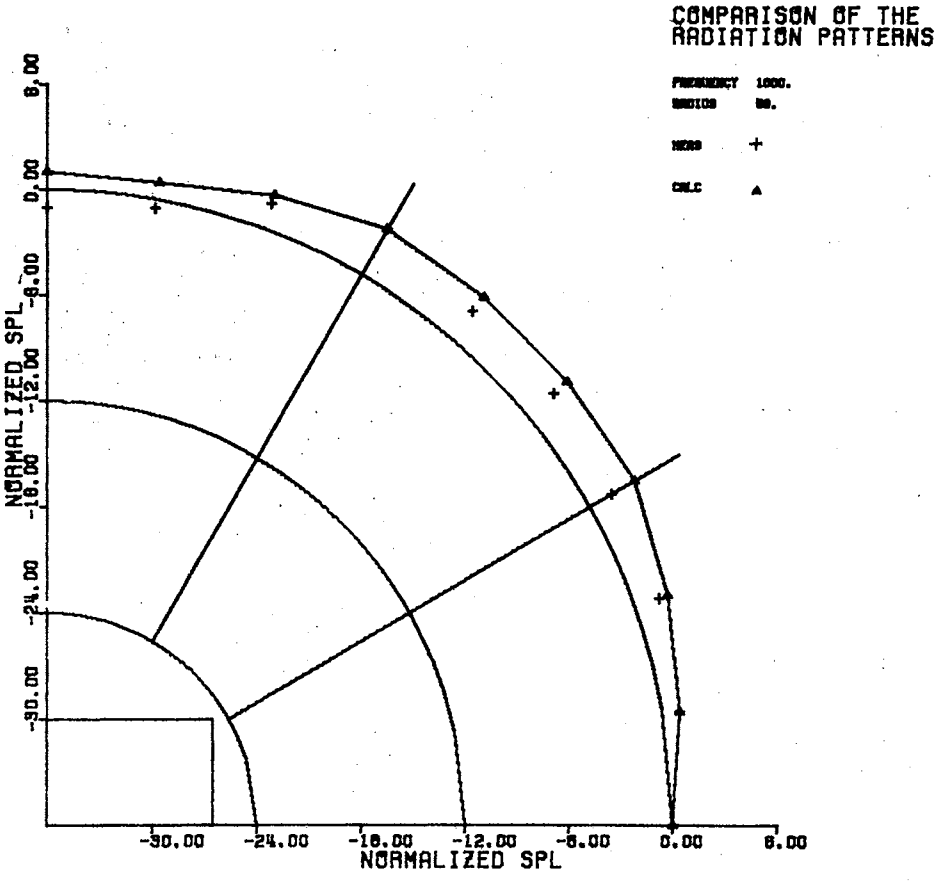

Figure 52. Comparison of Predicted and Measured Directivity Patterns

CHAPTER V

COMPARISON WITH OTHER METHODS

The preceding chapter gave the results of this research in the form of SPL versus distance curves and sound radiation patterns. A method was also proposed for obtaining an engineering estimate of noise radiation behavior based on the results of this data and the accuracy of this method was shown. This chapter will provide, for comparison, the estimates from some of the methods proposed in the literature. For purpose of this comparison an equilateral source with eight foot sides was used. As none of the other proposed methods are frequency dependent, an A-weighted SPL of 83.5 db measured at the surface of the large scale models was used. The estimates were all made for a distance of 24 feet, unless otherwise stated.

Rathe's method was only for estimating the SPL decrease with distance with a three slope asymptotic curve, which for this example reduced to two slopes since the source sides were of equal length. The curve break point was $8/\pi$ which gave an estimated SPL decrease of 20 db (to 63.5 db) and was within two db lower of the actual measured "A" level SPL. It was noted, however, that if the noise was predominantly in the 250 Hz octave band this estimate would be

10 db low, and if it was in the 4000 Hz band the estimate would be 6 db low at distances of 100 feet and greater. Ellis' correction to Rathe's method was negligible in this case.

Ellis' method was for estimating the SPL on the ground plane, and was primarily used here to determine the directivity pattern it predicts. The db corrections to be applied to the surface intensity were calculated and are tabulated in Table IV below.

TABLE IV

DB CORRECTIONS BY ELLIS' METHOD

Location (distance of 24')	Db Correction
Normal to center of surface	-14.7
Normal to edge of surface	-14.8
10° from normal to edge	-15.0
20° from normal to edge	-15.4
30° from normal to edge	-15.9
40° from normal to edge	-16.6
50° from normal to edge	-17.5
60° from normal to edge	-18.7
70° from normal to edge	-20.4
80° from normal to edge	-23.3
90° from normal to edge	-51.1

The above estimate for the db correction to be applied normal to the wall center on axis was about five db higher (conservative) than actually measured so would probably be acceptable. When two such plane radiating surfaces as tabulated above were positioned at right angles to simulate two walls of a building, and the above figures combined (by db addition), the resulting radiation pattern was a quarter circular arc around the corner, within ±1 db. In summary, after all the calculations, the estimate only indicated that all points equidistant from the surface have equal SPL's. The error involved in this estimate was obvious.

Tatge's proposed method was very simple to apply but as with Rathe's method, it was only good for estimating the SPL versus distance behavior. Actually there was no procedure to this method other than reading the SPL decrease directly from a series of curves plotted against distance which was normalized by the largest source dimension. For the particular example chosen, a 17 db decrease was read which was within three db (conservative) of the actual measurement, however, exactly the same errors were incurred as with Rathe's method (e.g. a ten db error at closer distances in the 250 Hz octave band, and a six db error at greater distances in the 4000 Hz octave band). The most serious error found in Tatge's paper after close scrutiny was that his curves indicated the farfield minus six db slope was obtained in every case at one wall width which was positively determined not to be the case by this research.

The last proposed method with which this research data was compared was Maekawa's. As stated in the introduction, this method was asserted to be valid at close distances and indeed the absolute limit was one and one half wall widths away from the surface, or 12 feet for our example. The data tabulated below in Table V for a single eight foot square plane surface was calculated from Maekawa's paper, using his equations and charts.

TABLE V

DB CORRECTIONS BY MAEKAWA'S METHOD

Location (distance of 12')	Db Correction
Normal to center of surface	- 4.0
Normal to edge of surface	- 5.2
22.5° from normal to edge	- 7.0
30	-10.0
45	- ∞

Of course it was immediately obvious that the combination of two such sources at right angles, as before would produce a major lobe on each axis with a 0 db cusp at 45 degrees, and absolutely no indication of any corner lobes as were actually measured.

It was then concluded that none of the existing methods known can yield a satisfactory engineering estimate of the sound radiation behavior measured during this research.

CHAPTER VI

SUMMARY, CONCLUSIONS AND RECOMMENDATIONS

An experimental study of the noise radiation behavior from three-dimensional rectangular sound sources was conducted to determine the influence of geometry, independent of dynamic characteristics. The sound-pressure level reduction with distance was measured in addition to the sound directivity patterns. The study included investigation of small scale acoustic models, large scale acoustic models and water table models. The length to width ratios of the models studied was from .5 to 2.

The data resulting from the study was compared with estimates obtained by use of methods proposed in the current literature by other authors.

A method was developed for estimating the sound pressure level versus distance plot for a practical three-dimensional noise source by use of normalized plots of the data gathered during this research. In addition, a method was proposed for estimating the directivity pattern around such a source by treating it as a "telescoping" pair of standard equilateral sources expanded to the desired length.

The following significant results were obtained during the study:

(1) The existence of acoustic lobes extending radially from the corners of rectangular sound sources was determined, with intensities several db greater than the intensity on the axis of symmetry. The magnitude and position of the lobes varied with the frequency band.

(2) Very good agreement was obtained between the directivity data of the small scale model experiments and the large scale model experiments when the frequency was scaled inversely to the model scale per normal procedures.

(3) The existence of the corner lobes was verified visually by use of surface wave generators and a water table, within the same source size to wave length ratios.

(4) The farfield behavior of SPL with distance was found to be very dependent on the frequency band of the sound. It was determined to be consistent, however, within a given frequency band between all sizes of the large scale models and the small scale models when normalized with a suitable parameter.

(5) Very poor agreement was generally found between the predictions obtained from the methods proposed by Rathe, Ellis, Tatge and Maekawa and the actual measured data.

Errors in the farfield estimates were 10 db in some cases, and none of the methods predicted any type of sound reinforcement at the corners to form lobes such as were measured.

(6) The acoustic corner lobes of all the models were able to be approximated very closely with smoothed data from the equilateral model source. The approximation derived from the use of the standard directivity pattern was generally within ±2 db.

The major conclusions drawn from this study are:

(1) There is a definite relationship between the geometry of a source and its sound directivity pattern, beyond the simple combination of the directivity patterns of its individual surfaces.

(2) Both the SPL decrease with distance and directivity patterns are strongly dependent on the frequency band of the noise, and therefore the frequency content of an anticipated noise source must be considered in any realistic attempt at predicting sound radiation behavior in a practical engineering situation.

(3) There was no method of satisfactorily estimating the SPL behavior with distance or the directivity patterns from three-dimensional rectangular sound sources. The

estimation methods for plane sources are all clearly inadequate for the three-dimensional case and the physical significance of a plane source is unclear at best.

(4) Any method that attempts to define farfield behavior of a general three-dimensional noise source in terms of a distance that has been normalized with only one of its three major dimensions will be in error, as the relationship is much more intricate.

(5) The procedures detailed in this study for estimating sound radiation behavior as a function of geometry and frequency band are very versatile tools. They are simple and straightforward to apply, but most important they provide a good conservative engineering estimate of noise radiation for many practical applications.

(6) Scale modeling is widely recognized as a relatively inexpensive and valuable tool in the study of architectural acoustics. It is just as valuable in the study of exterior noise radiation problems and is advisable in practical cases if a noise problem is anticipated. When lack of an anechoic facility prevents acoustic studies, water table studies could be considered as an alternative.

The following areas are recommended for future studies:

(1) It is first recommended that this study be expanded upon to confirm its validity for larger buildings, buildings of other construction and extreme proportioned buildings (e.g. very long and narrow, or very tall). As stated previously, this study encompassed models with length to width ratios of .5 to 2 and d/λ ratios of 1 to 60. Other shaped structures should also be the subject of future study, especially ones with an interior corner to determine their effect.

(2) Development of an accurate analytical model for a three-dimensional sound source is also recommended. The simplicity of applying the method described in this study makes it more desirable in the rectangular case but more intricate shapes may be able to be analyzed with an analytical model. A summary of the efforts in this study on an analytical model is contained in the appendix.

(3) A study of corner designs or special treatment that may be used to reduce the magnitude of the corner lobes is also encouraged. This study could even include landscaping schemes.

(4) Another area requiring study is a theory that will explain the existence of the corner lobes. As shown in this report,

the simple combination of two on-axis lobes does not produce the corner lobes. It appears that diffraction is not the explanation either as diffraction is predominant at low frequency and this lobe phenomena is predominant at high frequency.

BIBLIOGRAPHY

1. Skudrzyk, E. J. Simple and Complex Vibratory Systems. University Park, Pennsylvania, Pennsylvania State University Press, 1968.

2. Johnson, K. A., R. J. Ringlee, and M. W. Schulz, Jr. "Use of Scale-Models for Studying Power Transformer Audible Noise." Noise Control, Vol. 2, No. 2 (1956) pp. 54-60.

3. Ellis, R. M. "Cooling Tower Noise Generation and Radiation." J. of Sound and Vibration, Vol. 14 (1971), pp. 171-182.

4. Gosele, K. "Schallabstrahlung von Platten die zu Biegeschwingungen angeregt sind." Acustica, Vol. 3 (1953), pp. 243-248.

5. Cremer, L., and M. Heckl. Korperschall. Berlin, Springer-Verlag, 1967.

6. Rathe, E. J. "Note on Two Common Problems of Sound Propagation." J. of Sound and Vibration, Vol. 10 (1969), pp. 472-479.

7. Ellis, R. M. "The Sound Pressure of a Uniform, Finite, Plane Source." J. of Sound and Vibration, Vol. 14 (1970), pp. 503-508.

8. Tatge, R. B. "Noise Radiation by Plane Arrays of Incoherent Sources." JASA, Vol. 52 (1972), pp. 732-736.

9. Maekawa, Z. "Noise Reduction by Distance From Sources of Various Shapes." Applied Acoustics, Vol. 3 (1970), pp. 225-238.

10. Ingard, U. "On Sound-Transmission Anomalies in the Atmosphere." JASA, Vol. 45 (1969), pp. 1038-1039.

11. Weiner, F. M., and D. N. Keast. "Experimental Study of the Propagation of Sound over Ground." JASA, Vol. 31 (1959), pp. 724-733.

12. Ingard, U. "A Review of the Influence of Meteorological Conditions on Sound Propagation." JASA, Vol. 25 (1953), pp. 405-411.

13. Harris, C. M. "Absorption of Sound in Air Versus Humidity and Temperature." JASA, Vol. 40 (1966), pp. 148-159.

14. Beranek, L. L. Acoustics. New York, McGraw-Hill, 1954.

15. Beranek, L. L. Noise and Vibration Control. New York, McGraw-Hill, 1971.

16. Beranek, L. L. Noise Reduction. New York, McGraw-Hill, 1960.

17. Harris, C. M. Handbook of Noise Control. New York, McGraw-Hill, 1957.

18. Kinsler, L. E., and A. R. Frey. Fundamentals of Acoustics. New York, John Wiley & Sons, 1962.

19. Olson, H. F. Acoustical Engineering. Princeton, New Jersey, D. Van Nostrand, 1957.

APPENDIX A

Following is the list of equipment used during this study:

Small Scale Model Phase

1/4" Microphone, Bruel and Kjaer, Type 4136, S/N 277037

Frequency Analyzer, Bruel and Kjaer, Type 2107, S/N 224193

Graphic Level Recorder, General Radio, Model 1521, S/N 603

Random Noise Generator, General Radio, Model 1390-B, S/N 6517

Audio Amplifier, McIntosh, Model 75

VHF Driver, Electro-Voice, Model T350

Pistonphone, Bruel and Kjaer

RMS Voltmeter, Ballentine, Model 320

Large Scale Model Phase

1" Microphone, Bruel and Kjaer, Type 4131

Portable Sound Level Meter, Bruel and Kjaer, Type 2203

Octave-Band Filter Set, Bruel and Kjaer, Type 1613

Audio Oscillator, Hewlett-Packard, Model 200 AB

Loudspeaker System, Altec-Lansing, Model 1204-B

Water Table Phase

Audio Oscillator, General Radio, Model 1313 A

Audio Amplifier, Knight KB 30

Stroboscope, Chadwich-Helmuth, Model 127

Slip-Sync, Chadwick-Helmuth, Model 105 A

Model Construction

The small scale models were made of three-quarter inch plywood, with the sides beveled at 45 degrees and joined by gluing them solidly to form the 90 degree corners. The joints were then further sealed with putty to prevent leaks. No attempt was made to duplicate actual construction techniques.

The frame of the large scale model was constructed with two by four wooden studs on two foot centers, with the standard double stud at the corners. The one-half inch plywood was attached to the frame by eight penny nails with approximately one foot nail spacing. To facilitate expanding the model, the walls and insert sections were joined by bolts on two foot centers. All joints and corners were taped to seal acoustical leaks.

APPENDIX B

This appendix outlines the manner in which the equivalent frequencies for the water table experiments were obtained.

The important point to note is that the wave length of the surface gravity waves was the parameter of interest and not the wave length of the acoustic pressure waves in the water.

The range of acoustical wavelengths involved in the large scale model experiments varied from $\lambda_{250} = 4.53$ feet, to $\lambda_{4000} = .282$ feet. This gave a range of dimension to wavelength ratio for the 8 foot long model of:

$$\frac{8}{4.53} \leq \frac{d}{\lambda} \leq \frac{8}{.282}$$

$$1.77 \leq \frac{d}{\lambda} \leq 28.4$$

It was decided for practical reasons that the range of primary interest was between 1000 and 4000 hz which gave a new limit on the ratios as:

$$7.1 \leq \frac{d}{\lambda} \leq 28.4$$

The approximate velocity of gravity surface waves is given by:

$$C = \sqrt{gY}\left(1 + \frac{\Delta Y}{Y}\right)^{\frac{1}{2}}$$

Water depth was kept at approximately 1.6 inches and the wave amplitude was of .1 inch order of magnitude. Thus:

$$C \approx \sqrt{gY}$$

$$C \approx 25 \text{ inches/second}$$

Dimension of the wave generator was 6 inches, which dictated the range of wavelengths as:

$$\frac{6}{28.4} \leq \lambda \leq \frac{6}{7.1}$$

$$.21 \leq \lambda \leq .84$$

Obviously the frequency range of interest was given by:

$$\frac{25}{.84} \leq f \leq \frac{25}{.21}$$

$$29.8 \leq f \leq 119.2$$

or approximately 30 to 120 hz.

APPENDIX C

This appendix is a summary of the efforts at determining an analytical model for a three-dimensional rectangular sound source that would exhibit the same sound radiation behavior as measured in the study.

All efforts were directed at achieving a model for a single plane source that could be combined in a three-dimensional array with others to give similar directivity patterns to those measured. It was obvious that a plane source could not be satisfactorily modeled by any single, easily analyzed source such as a piston, pulsating sphere, or linear array of in-phase sources including a line source. The reason being that all of these sources of finite size have a major lobe on axis but no side lobes of sufficient magnitude to produce the corner lobes measured.

Examination of Cremer and Heckl's radiation patterns for linear arrays with opposite phasing (a series of dipoles) prompted the use of that type of model, with some success. First, a general m by n size array on each of two planes was programmed for the IBM 360 computer. This program added the RMS pressures (at any given radius) at every ten degrees azimuth from all the radiating

points on each surface, and at eleven frequencies in each octave band. It then averaged the pressures due to each of the eleven frequencies at the points on each azimuth. The roof was treated as being a source that radiated hemispherically, with an intensity equal to the average of the points on each azimuth pattern. This also served to smooth out the lobes and cusps in the pattern. Both the true average (mean) and RMS average were used with little difference in the results.

This general m by n array yielded a primary lobe with too great a magnitude plus too many secondary lobes to be satisfactory, so the model was then limited to a three by three array with much better success.

It was determined that a more satisfactory source model was obtained by placing the three by three array in the center of the plane surface with a certain spacing (ka) rather than spreading the array equally over the surface. An optimization search routine was used to determine the value of ka but the "surface" proved to be very complex and certainly not unimodal. Values of ka were determined for most cases that gave good approximations of the equilateral large scale model measured radiation patterns, but were generally unsatisfactory as the patterns were often too sensitive to ka (e.g. a change in ka of .1 in 10. changed the results significantly).

Examples of how closely this analytical model fit the data of the equilateral source is shown in Figures 53 through 56 for 500, 1000, 2000 and 4000 Hz, respectively. All of these estimates are acceptably close with the possible exception of 4000 Hz which is several db low at the lobes.

When the same analytical model was used to try to predict the directivity patterns of the elongated large scale-models, such close results were not achieved. It was still felt, however, that the success achieved makes this area worthy of further study.

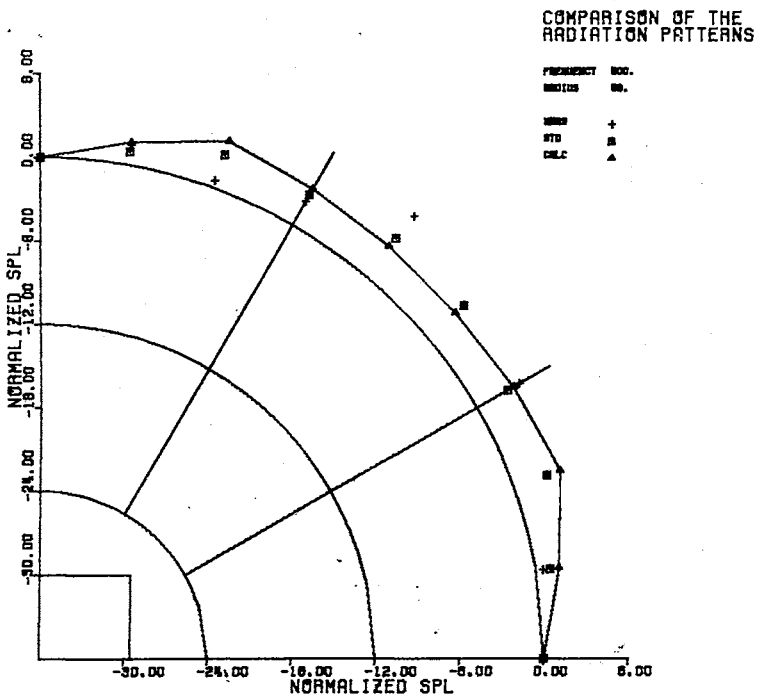

Figure 53. Analytical Model Directivity Pattern--500 Hz

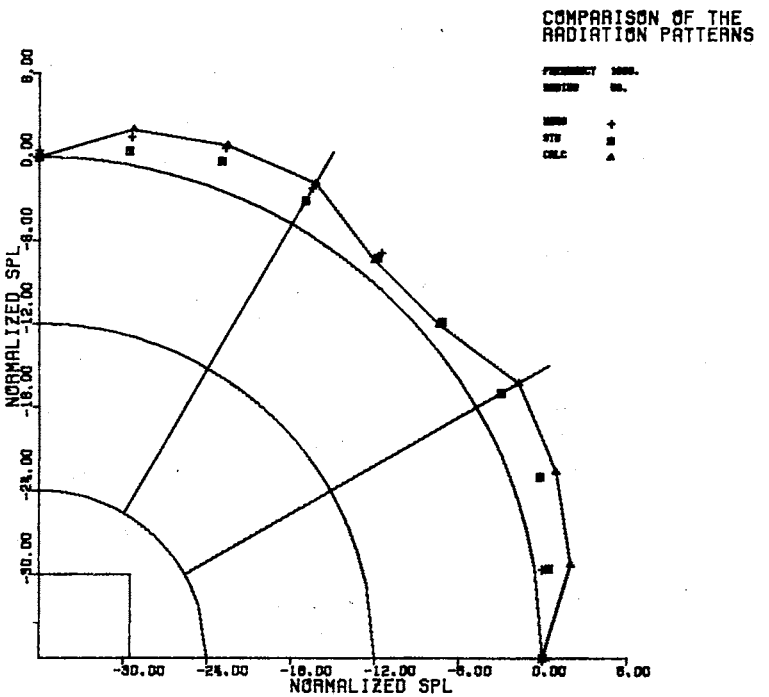

Figure 54. Analytical Model Directivity Pattern--1000 Hz

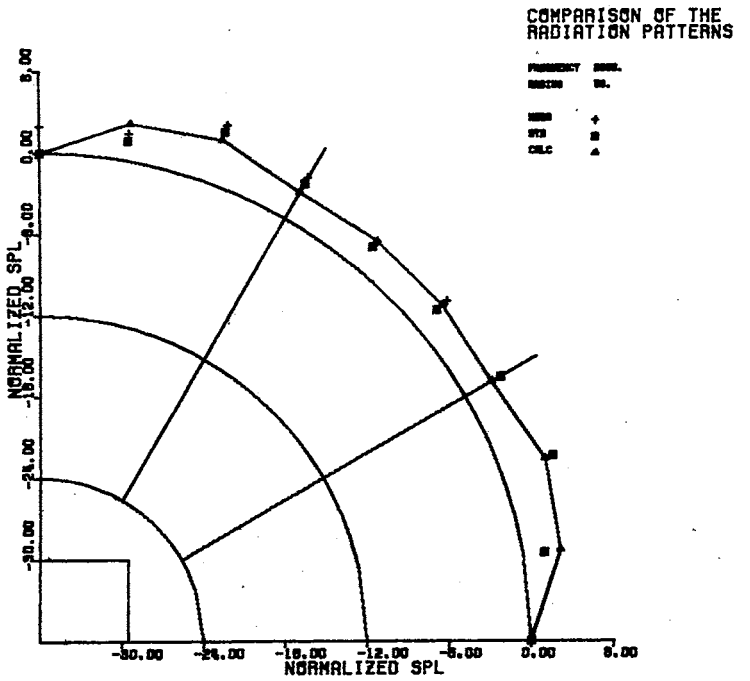

Figure 55. Analytical Model Directivity Pattern--2000 Hz

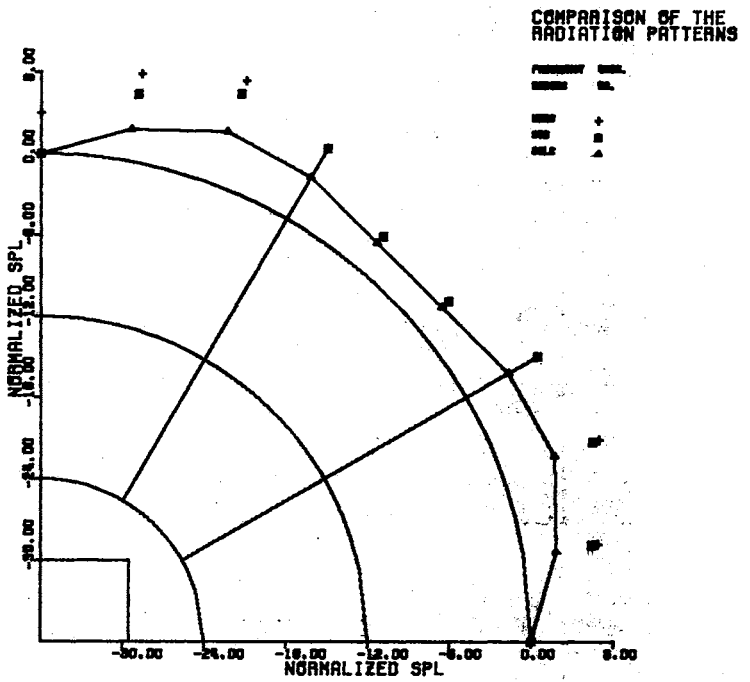

Figure 56. Analytical Model Directivity Pattern--4000 Hz

VITA[γ]

Grady Wayne Cook

Candidate for the Degree of

Doctor of Philosophy

Thesis: THE EFFECTS OF GEOMETRY ON SOUND RADIATION FROM THREE-DIMENSIONAL RECTANGULAR STRUCTURES

Major Field: Mechanical Engineering

Biographical:

Personal Data: Born December 24, 1937, in Oklahoma City, Oklahoma, the son of Mr. and Mrs. George W. Cook.

Education: Graduated from Will Rogers High School, Tulsa, Oklahoma, in May, 1955; received the degree of Bachelor of Science in Mechanical Engineering from Oklahoma State University, Stillwater, Oklahoma, in August, 1959; received the degree of Master of Science in Mechanical Engineering from Oklahoma State University in May, 1964; completed the requirements for the degree of Doctor of Philosophy from Oklahoma State University in May, 1973.

Professional Experience: Career United States Army Officer from August, 1959 to present, specializing in Research and Development; Project Engineer in the HAWK Missile Systems Project Managers Office, Redstone Arsenal, Alabama, from June, 1964 to August, 1966; Test Engineer in the Air Defense Systems Test Directorate, Aberdeen Proving Ground, Maryland, from August, 1967 to January, 1968; Project Engineer in the Detection and Sensor Laboratory, Mobility Equipment Research and Development Center, Fort Belvoir, Virginia, from October, 1966 to August, 1969.